TECHNICAL NOTES

NATIONAL ADVISORY COMMITTEE FOR AERONAUTICS

No. 856

EFFECT OF RIVET AND SPOT-WELD SPACING ON THE STRENGTH OF AXIALLY LOADED SHEET-STRINGER PANELS OF 24S-T ALUMINUM ALLOY

By Samuel Levy, Albert E. McPherson, and Walter Ramberg
National Bureau of Standards

Washington
August 1942

NATIONAL ADVISORY COMMITTEE FOR AERONAUTICS

TECHNICAL NOTE NO. 856

EFFECT OF RIVET AND SPOT-WELD SPACING ON THE STRENGTH OF AXIALLY LOADED SHEET-STRINGER PANELS OF 24S-T ALUMINUM ALLOY

By Samuel Levy, Albert E. McPherson, and Walter Ramberg

SUMMARY

Eighteen 24S-T aluminum-alloy sheet-stringer panels were tested in end compression under carefully controlled edge conditions. The stringers were fastened to the sheet by brazier-head rivets spaced 0.5 inch to 6 inches between centers for nine of the panels, by spot welds spaced 0.5 inch to 4 inches between centers for six of the panels, and by round-head rivets spaced 0.5 inch to 2 inches between centers for the other three panels.

In the tests of the panels with stringers fastened to the sheet by brazier-head rivets and by spot welds, measurements were made of the stringer strains and of the buckling deflections of the sheet. In the tests of the three panels with round-head rivets only the buckling loads and ultimate loads were measured.

The buckling load and the deflection of the sheet between rivets and spot welds were compared with Howland's theory. The buckling load of the sheet between stringers and the deflection of the sheet between stringers were compared with Timoshenko's theory. Most of the observed buckling loads and deflections were in agreement with these theories and indicated that the two types of buckling were substantially independent of each other for the specimens tested.

Four of the panels with brazier-head rivets and three of the panels with spot welds failed by separation of rivets or spot welds at stringer stresses of 24.2 to 39.5 kips per square inch. The other panels failed by stringer instability at a stringer stress between 37.0 and 42.0 kips per square inch.

The observed effective widths of the sheet between

stringers were from 8 percent lower to 20 percent higher than those calculated from Marguerre's approximate formula up to an edge strain at which buckling occurred between rivets or spot welds. The sheet load remained approximately constant after buckling of the sheet between rivets or spot welds.

A nomogram was devised for calculating the load for failure by stringer instability of panels of the type tested as a function of rivet or spot-weld spacing, stringer spacing, reinforcement ratio, and critical stringer stress.

For the 11 panels that failed by instability of the stringers the observed strengths at failure were within 6 percent of those calculated from the nomogram; for the seven panels that failed by rivet and spot-weld fracture the observed strengths were from 2 to 24 percent below the calculated values for stringer instability. The estimated loss in strength because of failure of rivets or spot welds exceeded 6 percent for only two panels for which the average sheet stress at failure was between 10.0 and 25.0 kips per square inch. No significant differences were found in the strength of panels fabricated with brazier-head rivets, spot welds, or round-head rivets.

INTRODUCTION

The strength of sheet-stringer panels in end compression has become a problem of importance with the increasing use of stiffened sheet to carry compressive loads in box beams for airplane wings and in other types of monocoque construction. In view of the importance of this problem the Bureau of Aeronautics, Navy Department, is supporting a long-range program on tests of sheet-stringer panels under carefully controlled edge conditions; the test program is being conducted at the National Bureau of Standards.

The first portion of this research program, consisting of an experimental study of deformation and effective widths of axially loaded sheet-stringer panels, was published as reference 1.

The second portion of this program, which is described in this paper, had the following objectives:

1. To determine the effect of the spacing of the

stringers and the spacing of the fastenings, rivets, or spot welds, on the strength of the panel

2. To compare the strength of panels fastened by spot welds, brazier-head rivets, and round-head rivets

3. To investigate the buckles, both elastic and permanent, in the sheet between fastenings and between stringers.

The authors are indebted to the Navy Department for permission to publish this work as a restricted paper.

APPARATUS AND TESTS

Panels

The dimensions of the panels are given in table 1 and in figure 1. The stringers, the sheet, and the rivets were 24S-T aluminum alloy. The stringers were nominally of the same dimensions for all the panels. Actually they varied between a cross-sectional area of 0.183 and 0.193 square inch.

The first nine panels listed in table 1 have stringers and sheet fastened by brazier-head rivets. The nominal ratios of stringer spacing to sheet thickness (b/t) are 20, 40, and 160, and the nominal ratios of fastening spacing to sheet thickness (L/t) are 20, 40, and 80. These ratios were chosen to give all combinations of buckling between stringers and between fastenings varying from buckles between stringers but not between fastenings for panel 7 $\left(\frac{L}{t} = 20.1, \frac{b}{t} = 161\right)$ to buckles between fastenings but not between stringers for panel 3 $\left(\frac{L}{t} = 76.1, \frac{b}{t} = 19.0\right)$.

To determine the effect of other fastenings on the strength, there were included panels 10 to 12, fastened by round-head rivets and panels 13 to 18 fastened by spot welds.

Mechanical properties of sheet and of stringers.- Tensile tests and pack compressive tests were made of

specimens from the sheet used in the panels. The resulting stress-strain curves are given in figure 2 and the mechanical properties are given in table 2.

One stringer (cross-sectional area = 0.194 sq in.) was cut into several specimens to determine the effect of length on the compressive strength. The specimens were cast in Wood's metal to a depth of 3/8 inch at each end. (See fig. 3.) Figure 4 shows the specimens after failure and figure 5 shows the ultimate loads and the loads corresponding to the yield strength. The loads corresponding to yield strength were obtained by the 0.2-percent-offset method from the compressive stress-strain curves. It is evident that a 4-inch length was sufficiently short to prevent instability before the yield strength was reached. Four-inch lengths accordingly were used to determine the compressive properties of the nine lengths of stringer stock used in the panels. Figure 3 shows six of these specimens after test and figure 6 shows the resulting nine compressive stress-strain curves. The mechanical properties are given in table 3.

Mounting panels in testing machine.- The panels were mounted in the testing machine after the ends had been ground flat and parallel in order to obtain uniform loading of sheet and stringers. The sheet was centered on ground steel blocks A (fig. 7) with the centroid of the specimen near the center of the blocks and was held in this position by tension rods H attached to the ends of the blocks. Crinkling failure of the sheet at the ends was prevented by forming a mold around the block and casting Wood's metal to a depth of about 1/4 inch around the end of the specimen. The castings were rigidly attached to the blocks by keys formed by the metal flowing into 1/4-inch holes inclined 15° from a perpendicular to the surface of the block. The specimen was then centered on the platen B of the testing machine and the tension rods were loosened. A plaster cap C about 1/8 inch thick was placed between the top block and the head of the testing machine to assure uniform bearing of the head against the block.

The edges of the sheet were supported laterally by two pairs of bars D (fig. 7) approximating the support of the sheet at the stringers. (See reference 1, p. 5.) Details of construction of these bars are shown in figure 8. The bars were separated by spacers the thickness of the sheet. Clearance between the spacers and the sheet permitted expansion of the sheet under load. For the pan-

els with fastening spacing equal to or less than the stringer spacing the bars were assembled as shown in figure 8(a). For the panels with fastening spacing greater than the stringer spacing the bars were assembled with localized supports on the sheet side of the panel to simulate the support given by the fastening at the stringers. These supports are shown at E in figure 9 and in figure 8(b).

The edge-support bars D were bolted to the spreader bars F (fig. 7) and the assembly, D and F, was supported on two pieces of sponge rubber G. The clearance between the ends of the bars D and the Wood's metal did not exceed 1/8 inch.

Strain measurements.- Pairs of strain gages were attached to only the stringer side of the panel and the sheet side was left free for deflection measurements. The extreme-fiber strains on the outstanding flanges of the stringers were measured by 2-inch Tuckerman strain gages (A, fig. 10). The strain in the stringer flange adjacent to the sheet was measured with the aid of Meisse transfers (reference 2) and strain gages shown in more detail in figures 11 and 12. "Hold-down" forces only were applied to the transfer by the harness B (figs. 10 and 11) attached to the flange of the stringers by small hook bolts C and C'. Bolts C were tightened snugly while bolts C' were tightened only enough to hold the harness against the stringer. The effect of the harness on the strength of the panels is believed to be negligible. Examination of the panels after test showed no tendency to fail outside the region between C and C' (fig. 11) at which the harness exerts the maximum restraint.

On the assumption that the strain varies linearly with the distance from the sheet, the average strain ϵ in the stringer was computed from the measured strains ϵ_1 and ϵ_2 (see fig. 13) by the formula

$$\epsilon = \epsilon_1 + \frac{c/2}{c-h} (\epsilon_2 - \epsilon_1) \qquad (1)$$

Substitution of the numerical values given in figure 1 gives

$$\epsilon = \epsilon_1 + 0.533 (\epsilon_2 - \epsilon_1) \qquad (1a)$$

Similarly, the strain ϵ' in the flange adjacent to the sheet was computed by the formula

$$\epsilon' = \epsilon_2 + \frac{h}{c-h}(\epsilon_2 - \epsilon_1) \qquad (2)$$

which gives

$$\epsilon' = \epsilon_2 + 0.0666\ (\epsilon_2 - \epsilon_1) \qquad (2a)$$

Deflection measurements.- The lateral deflection of the sheet midway between rivets along a stringer was measured by use of the gage shown in figure 9. The bar O had a conical seat at P and a longitudinal groove seat at Q for locating the gage on adjacent rivets, as shown in figure 14. There was a dial micrometer M midway between the seats. To detect any change in the gage, readings were taken on the standard bar S. The differences in these readings during a test did not exceed 0.001 inch. To locate the gage on spot welds, steel balls 1/8 inch in diameter were attached with cellulose nitrate cement, as shown in figure 15.

The lateral deflection of the sheet midway between stringers was similarly measured. Since the deflections of the sheet were measured midway between fastenings, they were not necessarily at the crest of the buckle between stringers.

Test schedule.- The panel was mounted in a vertical testing machine having a capacity of 100 kips. Strain gages were attached to the panels with brazier-head rivets (panels 1 to 9) and to the panels with spot welds (panels 13 to 18), and both stringer strains and deflection of the sheet between rivets or spot welds were read for small increases in load. The load was brought back to a low value at regular intervals to measure the permanent set in the stringers and in the sheet. Deflection of the sheet between rivets or spot welds was measured for panels 1, 2, 3, 4, 5, 6, 8, 9, 14, 15, 16, 17, and 18 and deflection of the sheet between stringers was measured for panels 7, 8, 9, 13, and 14. The deflection between rivets or spot welds was not measured for panels 7 and 13 because the deflection between stringers predominated in these panels. Deflection between stringers was not measured for panels 1, 2, 3, 4, 5, 6, 15, 16, 17, and 18 since the deflection between rivets (or spot welds) was predominant in these panels. Only the buckling and fail-

ing loads were observed for the panels with round-head rivets (panels 10, 11, 12).

RESULTS OF TESTS

Strains.- The load-strain graphs are shown in figures 16 to 30. The strains in the stringer are the average strain ϵ and the strains in the sheets are the strains ϵ', if it is assumed that the strain in the sheet is equal to the strain in the adjacent flange of the stringer. This assumption is justified if there is no slip in the rivets or the spot welds.

Deflections.- The graphs of strain against deflection along the stringers (figs. 31 to 43) and between the stringers (figs. 44 to 48) show a much better correlation between strain and deflection than between load and deflection because the deflection depended upon the strain in the adjacent flange of the stringer. Some of the small deflection readings were omitted to make the graphs clearer, but all the large deflections are shown.

Failure.- The ultimate load, the average sheet strain at failure (where measured), the average stress at failure, and the type of failure for the 18 panels are summarized in table 4.

Buckling of sheet between fastenings.- The elastic buckling of the sheet between fastenings has been calculated by W. L. Howland (reference 3) on the assumption that the lateral deflection is the same as that for a "fixed-end" Euler column of length equal to the fastening spacing and depth equal to the sheet thickness. On this basis the buckling strain is given by

$$\epsilon_c = \frac{\sigma_c}{E} = \frac{\pi^2 t^2}{3L^2} \qquad (3)$$

where

σ_c buckling stress

E Young's modulus

t sheet thickness

L fastening spacing

Equation (3) is plotted in figure 49 as curve A.

Above the proportional limit the buckling strains given by curve A are too high. This condition was corrected by replacing E with the combined modulus (reference 4 or 5) for the four sheet materials as calculated from the compressive stress-strain graphs in figure 2. The results are shown as curves B in figure 49.

Observed buckling strains were obtained from figures 31 to 43 as the intersection, with the strain axis of a curve through the points for large deflections. They are plotted in figure 49 for comparison with the calculated values. The point for $\frac{L}{t} = 19.0$ (panel 4) resulted from combined buckling between rivets and stringers in the plastic range. It was disregarded in drawing curve C. It is evident that both the panels with brazier-head rivets (curve C) and the panels with spot welds (curve D) buckle at strains somewhat lower than those calculated. A comparison of curves C and D indicates that the panels having spot welds (curve D) approach somewhat closer to the fixed-end condition (curve B) than do the panels having brazier-head rivets (curve C).

The deflection of the sheet between fastenings, the maximum stress in the sheet, and the strain at which the buckles became permanent were also estimated upon Howland's assumption that the sheet deflects like a fixed-end Euler column. The deflection y_f midway between fastenings is then given by

$$\frac{y_f}{t} = \frac{2}{\sqrt{3}} \sqrt{\frac{\epsilon'}{\epsilon_c} - 1} \tag{4}$$

where

ϵ' stringer strain at surface joining sheet and stringer (See equation (2a).)

ϵ_c buckling strain obtained from curves B (fig. 49)

The maximum stress σ in the buckled sheet is at the crest of the buckle on the stringer side of the sheet. It is given by

$$\frac{\sigma}{\sigma_c} = 1 + 2\sqrt{3} \sqrt{\frac{\epsilon'}{\epsilon_c} - 1} \tag{5}$$

It is assumed that the permanent set is appreciable when the maximum stress σ attains the yield strength σ_s (offset = 0.2 percent) of the material. The strain ϵ'_s for permanent set is then given by solving equation (5) for ϵ'

$$\frac{\epsilon'_s}{\epsilon_c} = \frac{1}{12}\left(\frac{\sigma_s}{\sigma_c} - 1\right)^2 + 1 \qquad (6)$$

In figures 31 to 43, the strain ϵ' is plotted against the theoretical deflection according to equation (4). (In fig. 39 the curve is off the paper.) For panels 2, 3, 5, 6, 9, 16, 17, and 18 the measured deflections were in rough agreement with the calculated deflections until yielding began in the sheet material. They were consistently larger than the calculated deflections for panels 1, 4, 14, and 15. In these panels the sheets buckled in the plastic range where the effect of initial eccentricity on the deflections is great (reference 5, p. 58). The negative deflections indicated buckling of the sheet toward the stringer. The negative deflections could not increase after the sheet was in contact with the stringer.

The theoretical strain ratio for permanent set according to equation (6) is plotted against the ratio of yield stress to buckling stress in figure 50. The observed points were plotted by using: for ϵ_c, the observed buckling strain (curves C and D in fig. 49); for σ_c, the corresponding stress as given by figure 2; for σ_s, the compressive yield strength as given by table 2; and for ϵ'_s, the strain estimated from figures 31 to 43 at which the permanent set in the buckles exceeded 10 percent of the total deflection. Panels 2, 4, 7, 9, 10, 11, 12, 13, and 17 had to be excluded from the comparison because no estimate of an experimental value of ϵ'_s could be made from the available data. The points in figure 50 for the other panels 1, 3, 5, 6, 8, 14. 15, 16, and 18 agree with the calculated curve (equation (6)) within the observational error for the strain for permanent set.

Typical buckles between fastenings are shown in figures 9, 15, 51, and 52. Buckles like those shown caused failure of the rivets (panels 1, 2, 4, and 5) or of the spot welds (panels 15, 16, and 17) for 7 of the 18 panels. In all except one of these panels the sheet strain at failure was much less than the sheet strain at failure

for the panels that failed by instability of the stringers. (See table 4.) It follows that failure of rivets or spot welds may reduce appreciably the strength of sheet-stringer panels.

In all of the cases of rivet failure and in some of the cases of spot-weld failure, the failure was accompanied by a loud report. In the other cases of spot-weld failure the weld gradually tore as the sheet peeled back from the stringer. Following the failures, the sheet and the stringer separated about 1/8 inch and, in the case of the spot welds, a hole was left in the sheet. This result indicated excessive tensile force just prior to failure and the need for adequate tensile strength in riveted or spot-welded joints.

A tensile force is set up by the prying action of the buckled sheet, as shown in figure 53. Outward buckling of the sheet started between rivets B and C. This outward buckling caused inward buckling between the adjacent pairs of rivets A and B and rivets C and D. The inward buckling was, however, restrained by the stringer, and the sheet remained nearly straight along AB and CD. Rivets B and C were subjected to a tensile force caused by the prying action of the buckled sheet, as well as to a bending moment and a shearing force. A numerical evaluation of these forces appears out of the question even within the elastic range.

An approximate analysis under simplifying assumptions was made, but this analysis led to a formula involving too many empirical constants to allow both the determination of the constants and the checking of the reliability of the formula from the data at hand. An estimate of the effect of rivet and spot-weld failure on the strength of the panels is given in a later section. This effect resulted in a loss in strength of 2 to 24 percent.

Deflection of sheet between stringers.— A theoretical value for the strain for buckling between stringers ϵ_{cr} was obtained upon the assumption that the sheet would buckle like an infinitely long plate of constant width and constant thickness the edges of which were clamped. The buckling strain may be expressed by a formula of the type proposed by Timoshenko (reference 5, p. 339)

$$\epsilon_{cr} = \frac{k \pi^2 D}{b^2 t E} \qquad (7)$$

$$D = \frac{E\,t^3}{12(1-\mu^2)}$$

where

D flexural rigidity of sheet

b stringer spacing

μ Poisson's ratio (0.3 for material)

The coefficient k for rigidly clamped edges is 7 (reference 5, p. 345).

The theoretical strain for buckling of the sheet between stringers was obtained from equation 7 by the use of the known dimensions of the panel and the elastic properties of the sheet. The theoretical and observed buckling strains for the panels that buckled between stringers before buckling between fastenings are given in table 5. The agreement is good for panels 7, 8, and 9. The calculated buckling strains for the other panels were in the plastic range for which this theory does not apply. It was felt that it would not be worth while to extend the theory to the case of plastic buckling because of the difficulty of adequately describing the initial eccentricity.

The deflection y_{st} of the buckles midway between stringers was calculated from the extension of Timoshenko's approximate theory as outlined in reference 1. A ratio of buckle width to buckle length of 1.49 was used corresponding to rigidly clamped edges. For panels 7, 8, and 9, t = 0.025 inch, $\epsilon_{cr} = 2.48\times10^{-4}$. Substituting these values in equation (14) of reference 1 gives:

$$y_{st} = \pm 0.0227\sqrt{4020\ \epsilon' - 1}\ \text{inch} \qquad (8a)$$

For panels 13 and 14, t = 0.051 inch; $\epsilon_{cr} = 41.7\times10^{-4}$. Substitution of these values in equation (14) of reference 1 gives

$$y_{st} = \pm 0.046\sqrt{240\ \epsilon' - 1}\ \text{inch} \qquad (8b)$$

Equations (8) are plotted in figures 44 to 48 for comparison with the observed deflections for panels 7, 8, 9, 13,

and 14. The observed deflections were bounded approximately by the theoretical crest values for panels 7 and 8. In the case of panel 9 the agreement was satisfactory up to a strain of 5×10^{-4} at which a change in buckle pattern occurred. (See fig. 52.) In panels 13 and 14 the sheet began to deflection plastically at a strain considerably below the theoretical strain for elastic buckling.

Effect of buckling on sheet load and effective width of sheet.- Buckling of the sheet between fastenings preceded buckling between stringers in panels 1, 2, 3, 5, 6, 16, 17, and 18. As mentioned in a previous section, the sheet was found to buckle like an Euler column. The sheet load would therefore be expected to remain nearly constant after buckling. This condition could be checked for panels 3, 6, 16, 17, and 18, in which buckling occurred between rivets or spot welds where the strain gages were attached. It was found that the sheet load for these panels remained fairly constant up to failure except for a small decrease after permanent set in the sheet buckles.

Buckling between stringers occurred first in panels 4, 7, 8, 9, 13, 14, 15. Marguerre's formula for effective width (reference 1, p. 45)

$$\begin{aligned} \frac{w}{b} &= 1 && \epsilon' \leq 3.64(t/b)^2 \\ \frac{w}{b} &= 1.54\left(\frac{1}{\epsilon'}\frac{t^2}{b^2}\right)^{1/3} && \epsilon' \geq 3.64(t/b)^2 \end{aligned} \tag{9}$$

was chosen for calculating the load in the sheet.

In figures 16 to 30 are drawn calculated curves, using a value of $E = 10.8\times10^6$ pounds per square inch and assuming that the load carried by the sheet is given by Marguerre's formula until buckling occurs between rivets or spot welds (curve B, fig. 49) and is constant afterward. It is seen that, except in the case of panel 17 (fig. 29), where the strain gages were partly over a buckled region and partly over an unbuckled region, the agreement between the calculated and the observed results is good up to stresses where yielding becomes appreciable.

The observed effective width w of the sheet was computed from the relation (reference 1, p. 39)

$$w = \frac{P_{sh}}{t\,\sigma_s} \tag{10}$$

where

P_{sh} sheet load

σ_s longitudinal compressive stress corresponding to strain ϵ' (fig. 2) on sheet side of stringer

The sheet load P_{sh} was calculated by subtracting the total load carried by the stringers from the applied load and dividing by 4 (corresponding to the four sheet bays). The load on each stringer was obtained from the average stringer strain (equation (1)), the compressive stress-strain curve of the stringer material (fig. 6), and the cross-sectional area of the stringer (table 1).

The observed effective widths for panels 7, 8, and 9 and for panels 13, 14, and 15 are plotted in figures 54 and 55, respectively. The calculated effective width according to Marguerre's formula (equation (9)) is plotted as a full line in these figures. The dashed curves were calculated on the assumption that the sheet load was constant after the sheet buckled between fastenings and was equal to the load just preceding buckling. In the elastic range this assumption leads to an effective width formula

$$\frac{w}{b} = \frac{w_c}{b} \frac{\epsilon_c}{\epsilon'} \tag{11}$$

where

w_c effective width according to equation (9) when $\epsilon' = \epsilon_c$

The observed effective widths were from 8 percent smaller to 20 percent greater than the calculated effective widths up to an edge strain at which buckling occurred between fastenings. The effective width after buckling was smaller than that given by Marguerre's formula (full line in figs. 54 and 55). Except for panels 14 and 15 immediately after buckling, it was greater than that calculated on the assumption of constant sheet load (dashed lines in figs. 54 and 55).

Strength of panels.- The strength of the panels that failed by stringer instability could be estimated as a function of the following quantities:

A total area of panel

r $\frac{\text{area of stringer}}{\text{total area of panel}}$

and of the stress–strain curves of the sheet and the stringer.

The load carried by the stringers was calculated as

$$P_{st} = r A \sigma_{st} \tag{12}$$

where σ_{st} is the stringer stress for instability.

The load carried by the sheet was calculated by applying the equations for effective width discussed in a previous section. In particular it was assumed that, before buckling occurred between rivets or spot welds, the sheet load could be calculated from Marguerre's effective-width formula (equation (9)) and that, after buckling occurred, the sheet load would be constant. With these assumptions the load carried by the sheet becomes:

$$P_{sh} = (1 - r) A \frac{w_c}{b} \sigma_c \tag{13}$$

where w_c is the effective width according to Marguerre's formula (equation (9)) corresponding to an edge strain ϵ_c or an edge stress σ_c; the relation between ϵ_c and σ_c is given by the longitudinal compressive stress–strain curves (fig. 2). The edge strain ϵ_c was chosen as the lowest one of the following two values: the strain corresponding to stringer instability or the strain corresponding to buckling between rivets according to curve C, figure 49. (Curve C was used for all the panels because it is slightly on the conservative side for the spot-weld panels and because there were no measurements for the round-head rivet panels.)

The total load on the panel is

$$P = P_{st} + P_{sh}$$

and the average stress in the panel is

$$\frac{P}{A} = \frac{P_{st}}{A} + \frac{P_{sh}}{A} \tag{14}$$

The solution of equation (14) for the average stress in the panel at failure may be conveniently obtained from the nomogram shown in figure 56. This nomogram was computed by using the average compressive properties of the

sheet and stringer in figures 2 and 6. If, for example, σ_{st}, L/t, b/t, and r are given, the procedure for determining P/A is as follows. From a given value of σ_{st} on scale I draw two lines: one line to scale III intersecting scale II at the given value of r, and the other line through point O intersecting scale I'. If the last-mentioned intersection is at a value on scale I' less than the given value of L/t, use the given value of L/t in the subsequent procedure; otherwise use the value at the intersection on scale I'. Draw a line between the given value b/t on scale XI and the proper value of L/t on scale X. From the intersection of this line with scale IX, or from 1 on scale IX in the case of no intersection, draw a line through the proper value of L/t on scale VIII. From the intersection of this line with scale VII, draw a line intersecting scale VI at the given value of r. Finally, from the intersection of this line with scale V draw a closing line to the intersection with scale III of the first line drawn. The intersection with scale IV of the line between scales V and III determines P/A. It may be noted that the intersections with scales III, V, VII, and IX determine the values at failure of P_{st}/A, P_{sh}/A, σ_{sh} (average), and w_c/b, respectively.

Scale IX in the nomogram gives the ratio of effective width to initial width of the sheet at the time of stringer instability or of buckling between rivets or spot welds; it cannot exceed 1 because the effective width cannot exceed the initial width. Scale I' gives values that should be used instead of L/t wherever L/t is less than the intersection on scale I', thus taking care of those cases where stringer instability occurs before buckling between fastenings.

The use of the nomogram will be illustrated by solving the following two examples:

Example 1:

σ_{st} = 39.5 kips per square inch $\quad \frac{L}{t} = 20$

$\frac{b}{t} = 80 \qquad r = 0.5 \qquad A = 1.5$ square inches

The solution is given by lines A – A in figure 56, as follows:

Draw a line through σ_{st} = 39.5 kips per square inch

on scale I and $r = 0.5$ on scale II, Draw a line through $\sigma_{st} = 39.5$ kips per square inch and the point 0 intersecting scale I'. Since the value at the intersection is less than 20, use $\frac{L}{t} = 20$ as directed. Draw a line through $\frac{b}{t} = 80$ on scale XI and $\frac{L}{t} = 20$ on scale X. Draw a line through the intersection of this line with scale IX and $\frac{L}{t} = 20$ on scale VIII. Then draw a line through the intersection of the last line with scale VII and $r = 0.5$ on scale VI. Connect the intersection of the line with scale V and the intersection of the first line with scale III. The connecting line intersects scale IV at $\frac{P}{A} = 30.1$ kips per square inch. The load at failure is therefore $P = 30.1\ A = 30.1 \times 1.5 = 45.1$ kips.

Example 2:

$\sigma_{st} = 45.0$ kips per square inch $\quad \frac{L}{t} = 40$

$\frac{b}{t} = 20 \quad r = 0.6 \quad A = 1.25$ square inches

The solution is given by line B — B in figure 56. The same procedure is followed as for example 1 except that, since the line drawn between scale XI and X does not intersect scale IX, the construction proceeds from 1 on this scale as directed. The solution is given by the intersection of B — B with scale IV at $\frac{P}{A} = 34.8$ kips per square inch or $P = 34.8 \times 1.25 = 43.6$ kips.

Panels 3, 6, 7, 8, 9, 13, 14, and 18 were tested with strain gages attached and failed by stringer instability at stringer stresses varying from 37.0 to 42.0 kips per square inch with an average value of 39 kips per square inch. The failing loads of these panels were computed from the nomogram on the assumption that the stringer stress at failure was 39 kips per square inch; they are plotted against the observed failing loads as open points in figure 57. The values for the panels that failed by separation of rivets or spot welds are shown on the same figure as full points.

Although 7 (1, 2, 4, 5, 15, 16, and 17) of the 18 panels failed in the rivets or spot welds, only 2 (2 and 16) of the panels failed at loads more than 6 percent below those estimated in the absence of failure of rivets or spot welds. In all seven of the panels that had rivet or spot-weld failures, buckling between fastenings preceded failure of the fastening. It seemed reasonable, therefore, that the strength of those panels having a high average sheet stress at the time of buckling was not materially reduced by failure of rivets or spot welds because the sheet already was carrying almost its maximum load. At the other extreme, it seemed reasonable that the strength of those panels having a low average sheet stress at the time of buckling would also not be materially reduced by failure of rivets or spot welds since in these cases the sheet would have to be quite flexible and could not exert a sufficient force on the rivet or spot weld to cause failure until the load on the panel was almost a maximum. Between the extremes of high and low average sheet stress there is probably an intermediate region for which failure of the fastenings may appreciably weaken the panel.

The existence of such an intermediate region is confirmed by figure 58 showing the ratio of observed failing load to calculated failing load and the average sheet stress at failure calculated from the nomogram, scale VII, figure 56. It is evident that outside the "danger zone," average calculated sheet stress between 10 and 25 kips per square inch, failure of fastenings did not cause a material reduction in the strength of the panels; although four of the seven failures of fastenings actually occurred outside this range.

Examination of scales VII to XI of the nomogram shows that the average sheet stress for failure by stringer instability of aluminum-alloy panels of this type is a function only of the ratios L/t and b/t (provided the ratio L/t is greater than the intersection on scale I'). The danger zone shown in figure 58 may be expressed as a function of these two ratios as indicated in figure 59. This figure is presented more as a guide in planning future tests than as a guide to designers of panels. The number of panels tested was not sufficient to define clearly the region in which serious weakening by rivet or spot-weld failures might occur.

Furthermore, it should be realized that figures 56,

58, and 59 are based only on tests of 24S-T aluminum-alloy panels with Z stringers. They cannot be safely applied without experimental confirmation to panels of other materials and with other types of stringer.

National Bureau of Standards,
Washington, D. C., October 1941.

REFERENCES

1. Ramberg, Walter, McPherson, Albert E., and Levy, Sam: Experimental Study of Deformation and of Effective Width in Axially Loaded Sheet-Stringer Panels. T.N. No. 684, NACA, 1939.

2. Meisse, L. A.: Improvement in the Adaptability of the Tuckerman Strain Gage. A.S.T.M. Proc., vol. 37, pt. II, 1937, pp. 650-654.

3. Howland, W. L.: Effect of Rivet Spacing on Stiffened Thin Sheet under Compression. Jour. Aero. Sci., vol. 3, no. 12, Oct. 1936, pp. 434-439.

4. von Kármán, Th.: Untersuchungen über Knickfestigkeit, Forschungsarbeiten, Heft 81, 1910.

5. Timoshenko, S.: Theory of Elastic Stability. McGraw-Hill Book Co., Inc., 1936.

TABLE 1.- DESCRIPTION OF PANELS
[See also fig. 1]

Panel	Cross-sectional area of panel (sq in.)	Cross-sectional area of each stringer (sq in.)	Length of panel, l (in.)	Width of panel, 4b (in.)	Thickness of sheet, t (in.)	Rivet or spot-weld spacing, L (in.)	b/t	L/t	Type of fastening
1	1.350	0.183	12.00	8.00	0.1001	2.00	20.0	20.0	Brazier-head rivet
2	1.354	.183	12.00	8.00	.1007	4.00	19.9	39.7	
3	1.051	.193	18.00	6.00	.0768	6.00	19.0	76.1	
4	1.522	.193	12.00	12.00	.0790	1.50	37.9	19.0	
5	.989	.193	11.99	8.00	.0511	2.00	39.1	39.1	
6	.992	.193	12.00	8.00	.0517	4.00	38.6	77.3	
7	.949	.184	12.00	16.00	.0248	.50	161	20.1	
8	.952	.184	11.96	15.99	.0250	1.00	160	40.0	
9	.948	.184	12.00	16.00	.0247	2.00	162	80.9	
10	.948	.184	11.99	16.00	.0247	.50	162	20.2	Round-head rivet
11	.979	.193	12.00	16.00	.0250	1.00	160	40.0	
12	.976	.193	12.00	16.00	.0248	2.00	161	80.6	
13	.982	.192	11.99	8.00	.0507	.50	39.4	9.9	Spot-weld
14	.978	.192	12.01	8.00	.0502	1.00	39.8	19.9	
15	.965	.185	11.96	8.00	.0512	1.50	39.0	29.3	
16	.967	.185	11.99	8.01	.0515	2.00	39.8	39.8	
17	.954	.185	11.99	8.00	.0499	3.00	40.0	60.1	
18	.959	.185	11.99	8.02	.0500	4.00	40.1	80.0	

TABLE 2.- TENSILE AND COMPRESSIVE PROPERTIES OF SHEET
[See also fig. 2]

Nominal thickness of sheet (in.)	Direction of load	Young's modulus		Yield strength (offset = 0.2 percent)		Tensile strength
		Tension (kips/sq in.)	Compression (kips/sq in.)	Tension (kips/sq in.)	Compression (kips/sq in.)	(kips/sq in.)
0.025	Longitudinal	10,400	10,700	53.5	45.5	71.6
.025	Transverse	10,400	-------	45.9	----	69.6
.052	Longitudinal	10,500	10,800	57.3	46.0	72.7
.052	Transverse	10,300	-------	45.5	----	69.0
.079	Longitudinal	10,400	10,800	53.5	44.9	71.9
.079	Transverse	10,500	-------	46.5	----	69.4
.100	Longitudinal	10,400	10,700	49.5	44.6	69.9
.100	Transverse	10,300	-------	45.1	----	67.3

TABLE 3.- COMPRESSIVE TESTS OF 4-INCH LENGTHS OF STRINGER STOCK USED IN THE PANELS

Used in panel	Cross-sectional area (sq in.)	Young's modulus (kips/sq in.)	Yield strength (kips/sq in.)	Ultimate strength (kips/sq in.)
1, 2	0.183	10,700	40.3	47.6
3, 4	.193	10,800	39.9	49.6
5, 6	.193	11,000	40.3	48.9
7, 8	.184	10,900	39.9	49.1
9, 10	.184	10,800	39.0	47.5
11, 12	.193	10,600	39.7	50.5
13, 14	.192	10,600	38.9	48.2
15, 16	.185	10,900	40.9	48.1
17, 18	.185	10,800	40.8	48.7

TABLE 5.- BUCKLING OF SHEET BETWEEN STRINGERS

Panel	L/t	b/t	Buckling strain	
			Calculated (a)	Observed
4	19.0	37.9	44.2×10^{-4}	[b] 25.5×10^{-4}
7	20.1	161	2.5	3.3
8	40.0	160	2.5	2.5
9	80.9	162	2.5	2.0
13	9.86	39.4	41.4	26.0
14	19.9	39.8	40.2	27.5
15	29.3	39.0	41.8	24.3

[a] Poisson's ratio = 0.3. Calculated on the assumptions that the plate remains elastic and that the edges are clamped.

[b] In the edge bays only.

TABLE 4.- FAILURE OF PANELS

Panel	Stringer area ÷ total area, $r = \frac{A_{st}}{A}$	Stringer spacing ÷ thickness, b/t	Rivet or spot-weld spacing ÷ thickness, L/t	Maximum load, P (kips)	Stress (average), P/A (kips/sq in.)	Stringer stress, σ_{st} (kips/sq in.)	Sheet strain (average), ϵ'	Type of failure
1	0.406	20.0	20.0	47.0	34.9	35.3	34.8×10^{-4}	Rivet
2	.404	19.9	39.7	29.0	21.4	24.2	19.9	
3	.550	19.0	76.1	24.6	23.4	38.5	62.0	Stringer
4	.379	37.9	19.0	49.1	32.2	34.7	29.1	Rivet
5	.587	39.1	39.1	29.4	29.7	39.5	60.0	
6	.583	38.6	77.3	25.4	25.6	40.2	60.0	Stringer
7	.581	161	20.1	27.3	28.9	42.0	55.0	
8	.579	160	40.0	25.3	26.6	38.0	50.0	
9	.582	162	80.9	23.8	25.1	38.7	55.0	
10	.583	162	20.2	27.1	28.6	———	———	
11	.591	160	40.0	27.2	27.8	———	———	
12	.593	161	80.6	26.1	26.8	———	———	
13	.567	39.4	9.86	34.8	35.5	37.0	49.0	
14	.588	39.8	19.9	33.2	34.0	37.0	52.0	
15	.575	39.0	29.3	30.8	31.9	35.7	39.5	Spot-weld
16	.574	39.8	39.8	26.1	27.0	34.7	38.5	
17	.581	40.0	60.1	23.5	24.7	35.1	28.0	
18	.578	40.1	80.0	23.9	25.0	40.1	55.0	Stringer

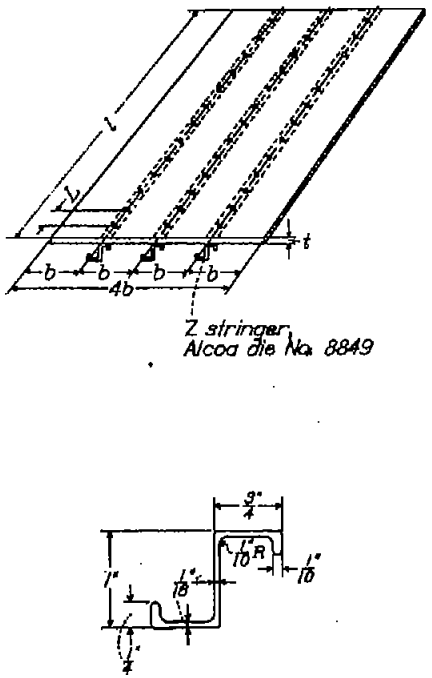

Figure 1.- Construction of sheet-stringer panels and nominal dimensions of stringer. Stringers fastened to sheet by 1/8-inch brazier-head rivets for panels 1 to 9; 1/8-inch round-head rivets for panels 10 to 12; and spot-welds with 1/4-inch indentation diameter for panels 13 to 18.

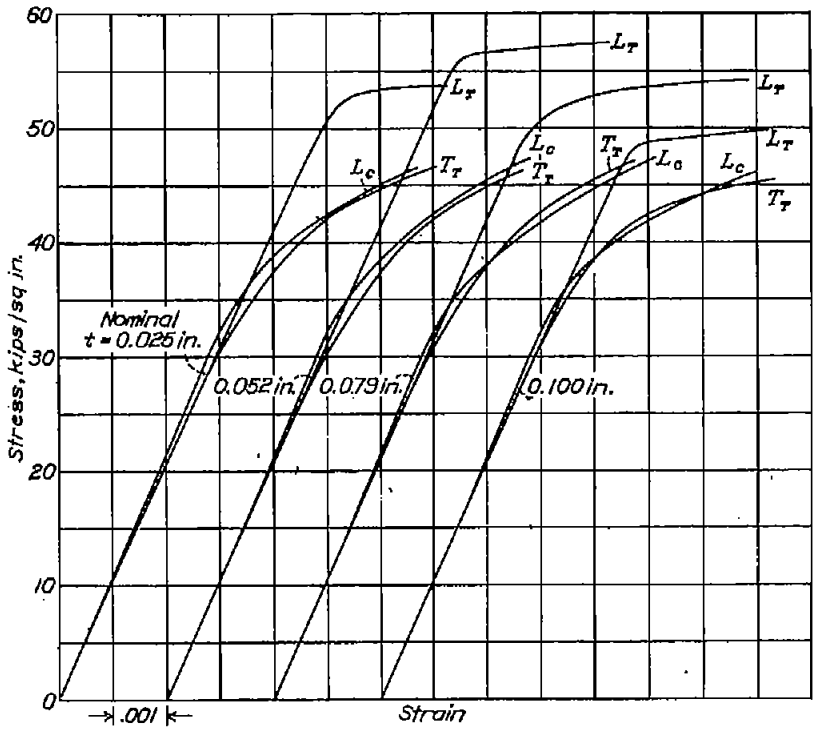

Figure 2.- Stress-strain curves of 24S-T aluminum-alloy sheet used in panels.

L_T tension in direction of rolling

L_C compression in direction of rolling

T_T tension transverse to direction of rolling

Figs. 1,2

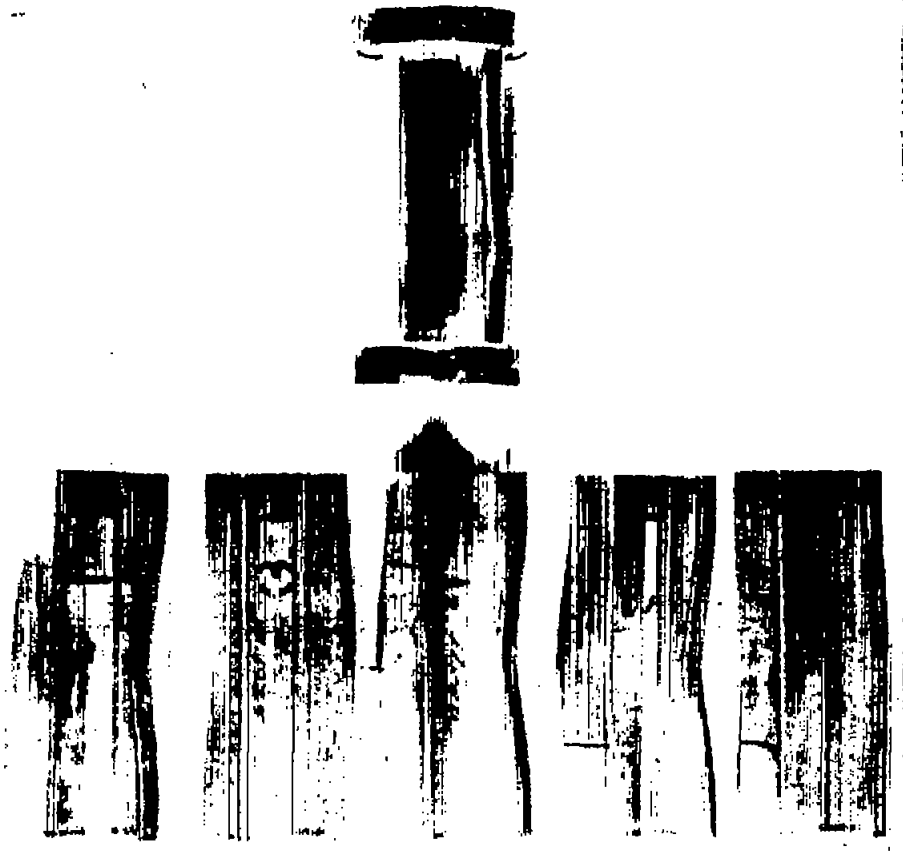

Figure 3.- Four-inch lengths of stringer after compressive test.

Figure 4.- The 2-,4-,6-,8-,12-, and 16-inch lengths of stringer after compressive test.

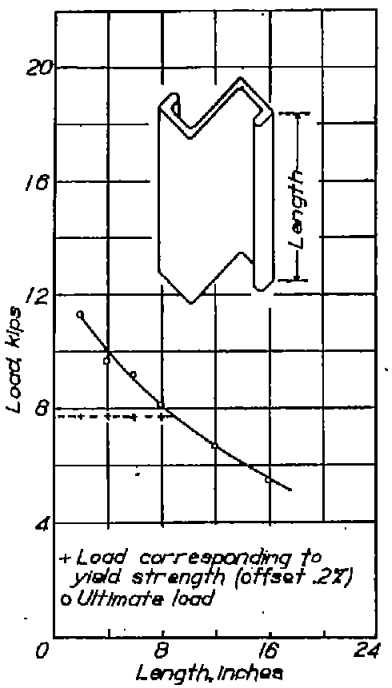

Figure 5.- Compressive tests of specimens cut from one length of Z-stringer, area = 0.194 sq in.

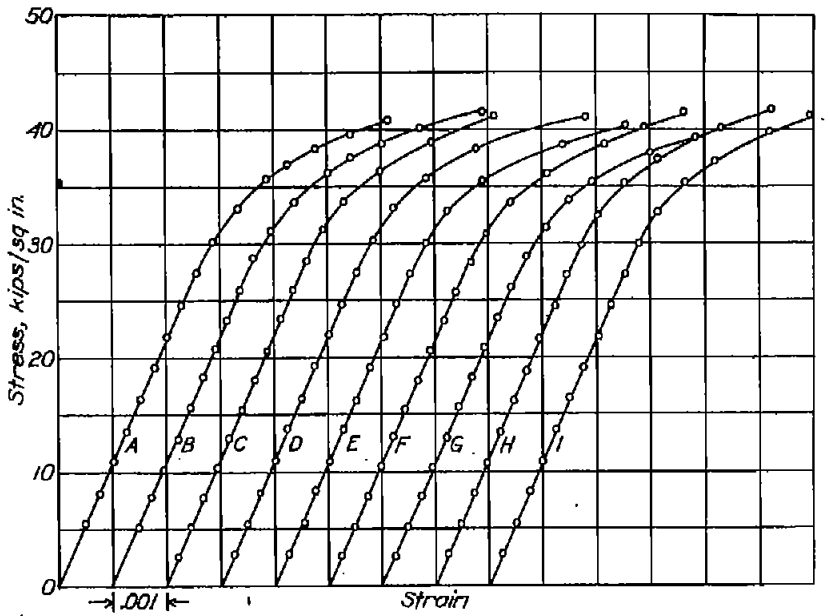

Figure 6.- Compressive stress-strain curves of four-inch lengths of Z-stringers; A, used in panels 1 and 2; B, used in panels 3 and 4; C, used in panels 5 and 6; D, used in panels 7 and 8; E, used in panels 9 and 10; F, used in panels 11 and 12; G, used in panels 13 and 14; H, used in panels 15 and 16; and I, used in panels 17 and 18.

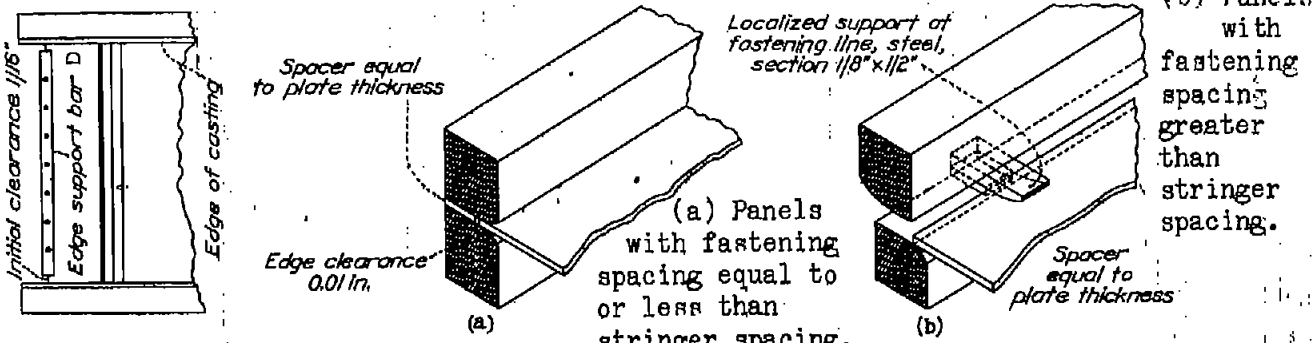

(a) Panels with fastening spacing equal to or less than stringer spacing.

(b) Panels with fastening spacing greater than stringer spacing.

Figure 8.- Edge supports.

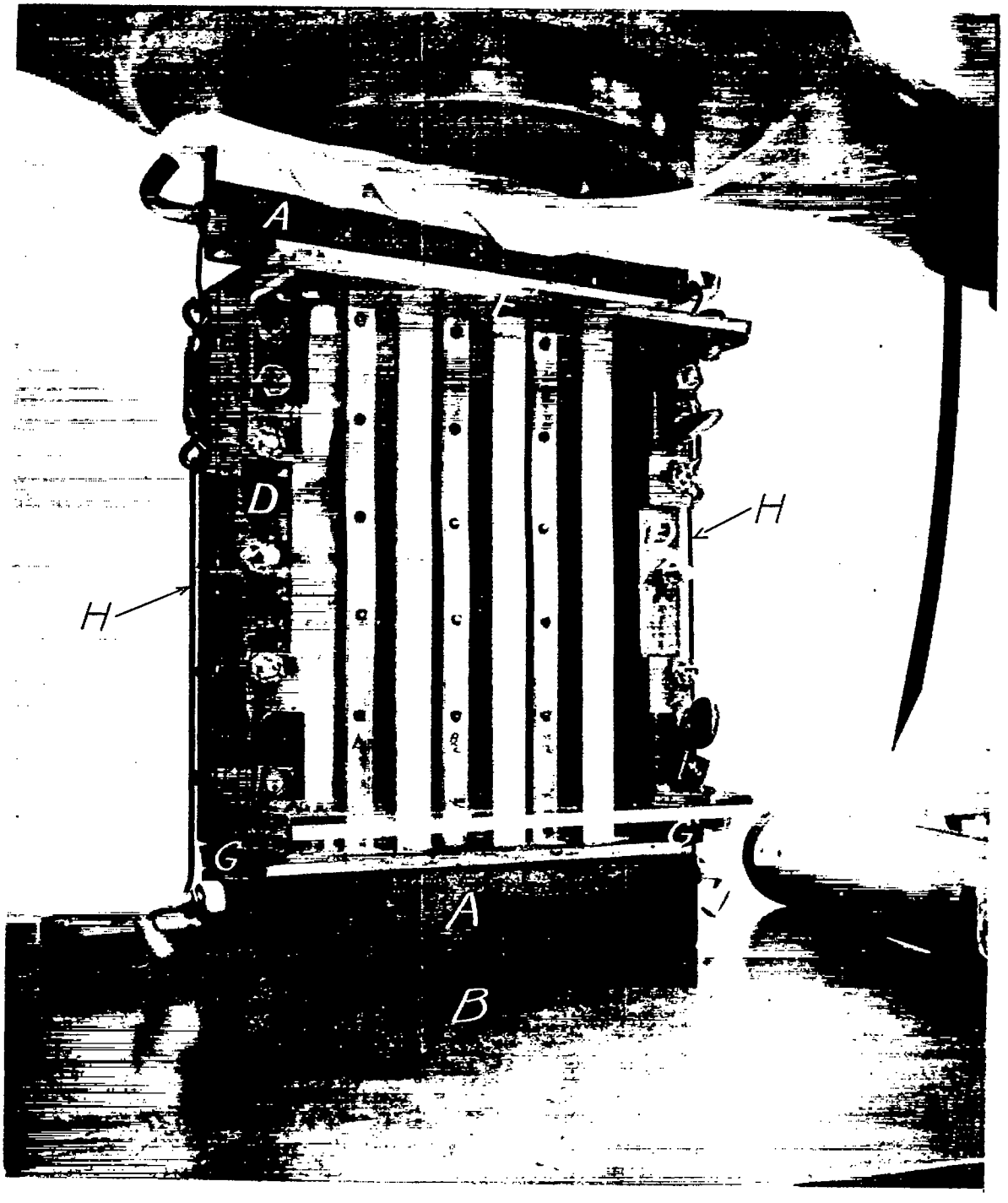

Figure 7. - Panel 1 after test.

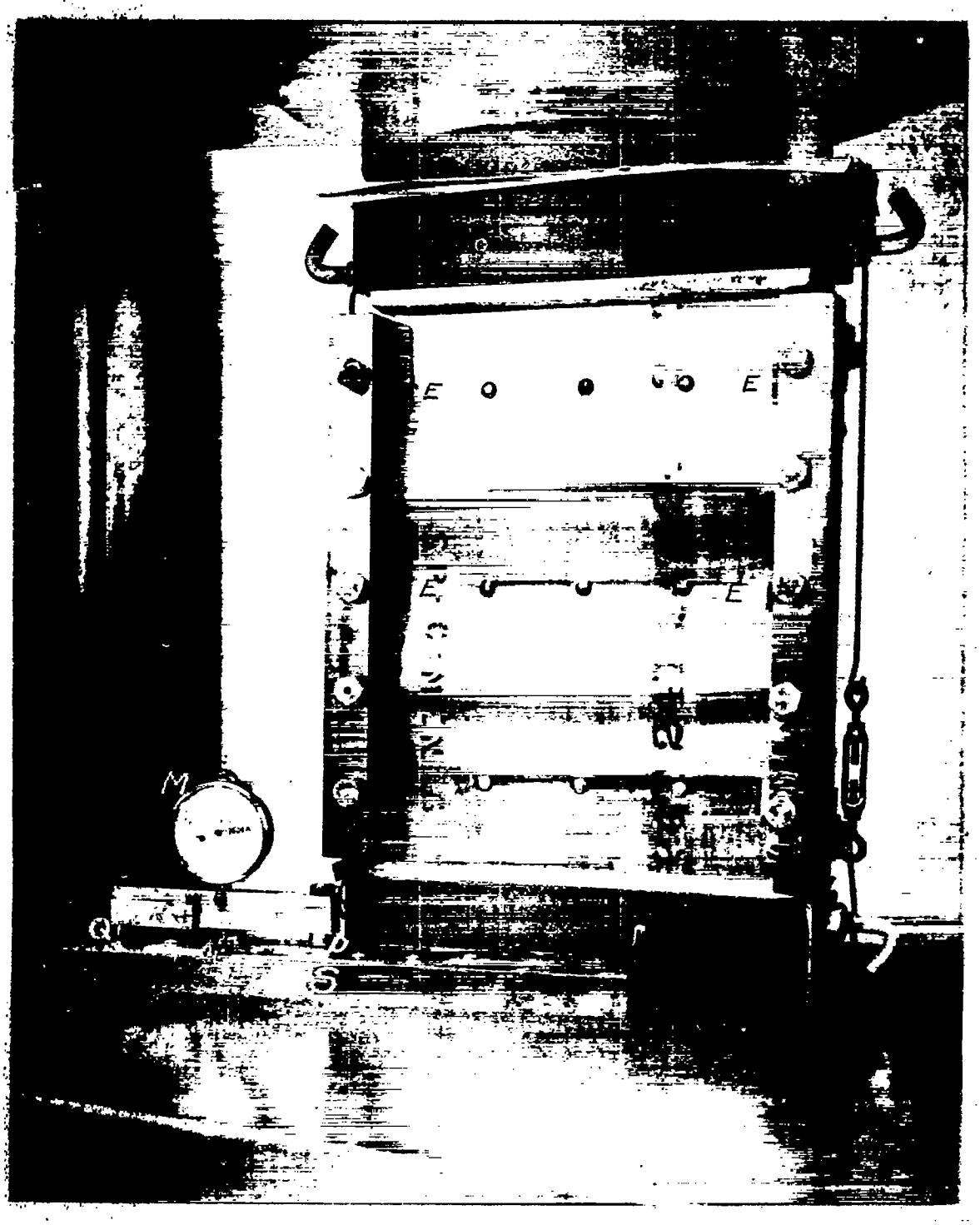

Figure 9. - Panel 6 after test.

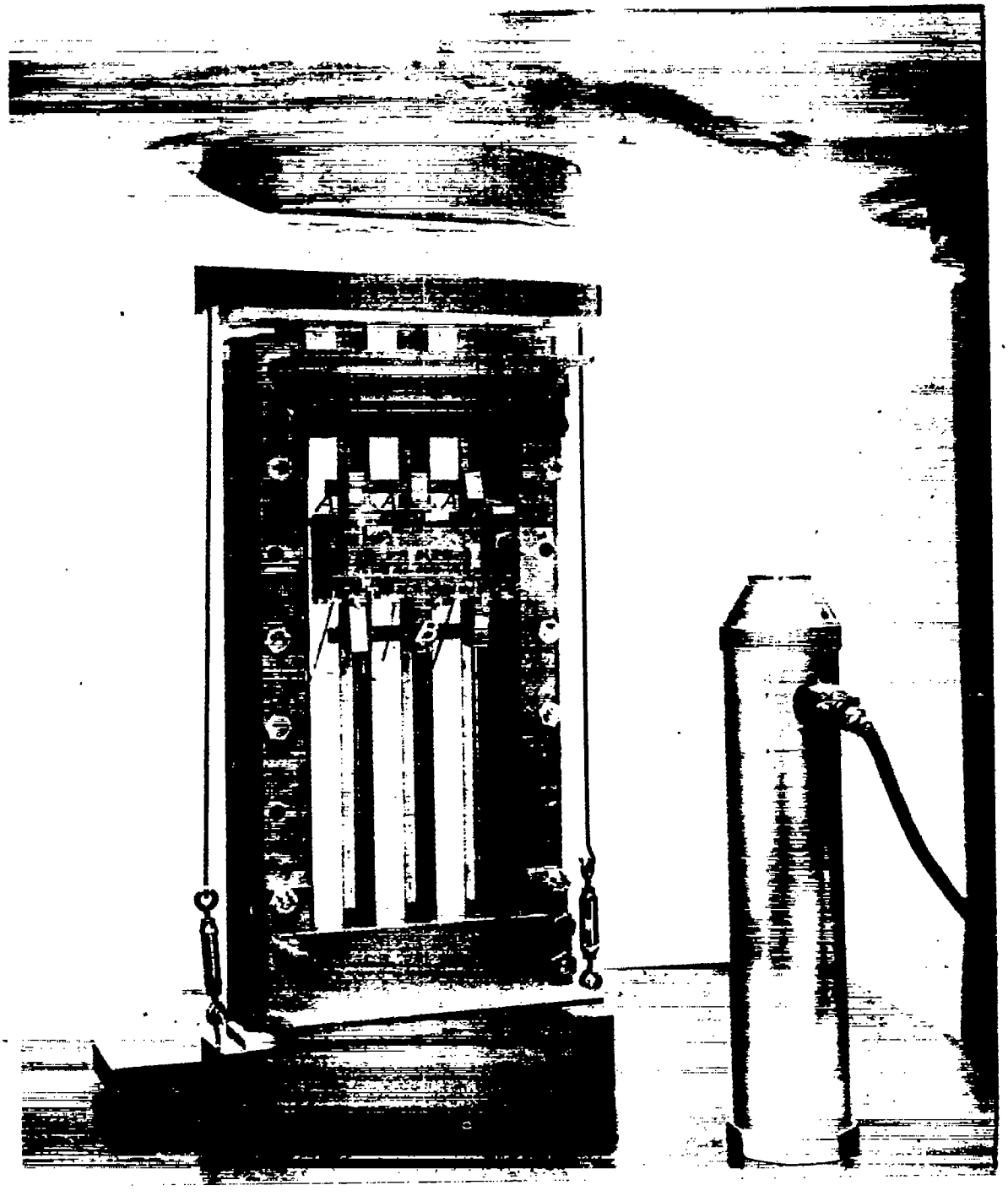

Figure 10. - Panel 3 before test.

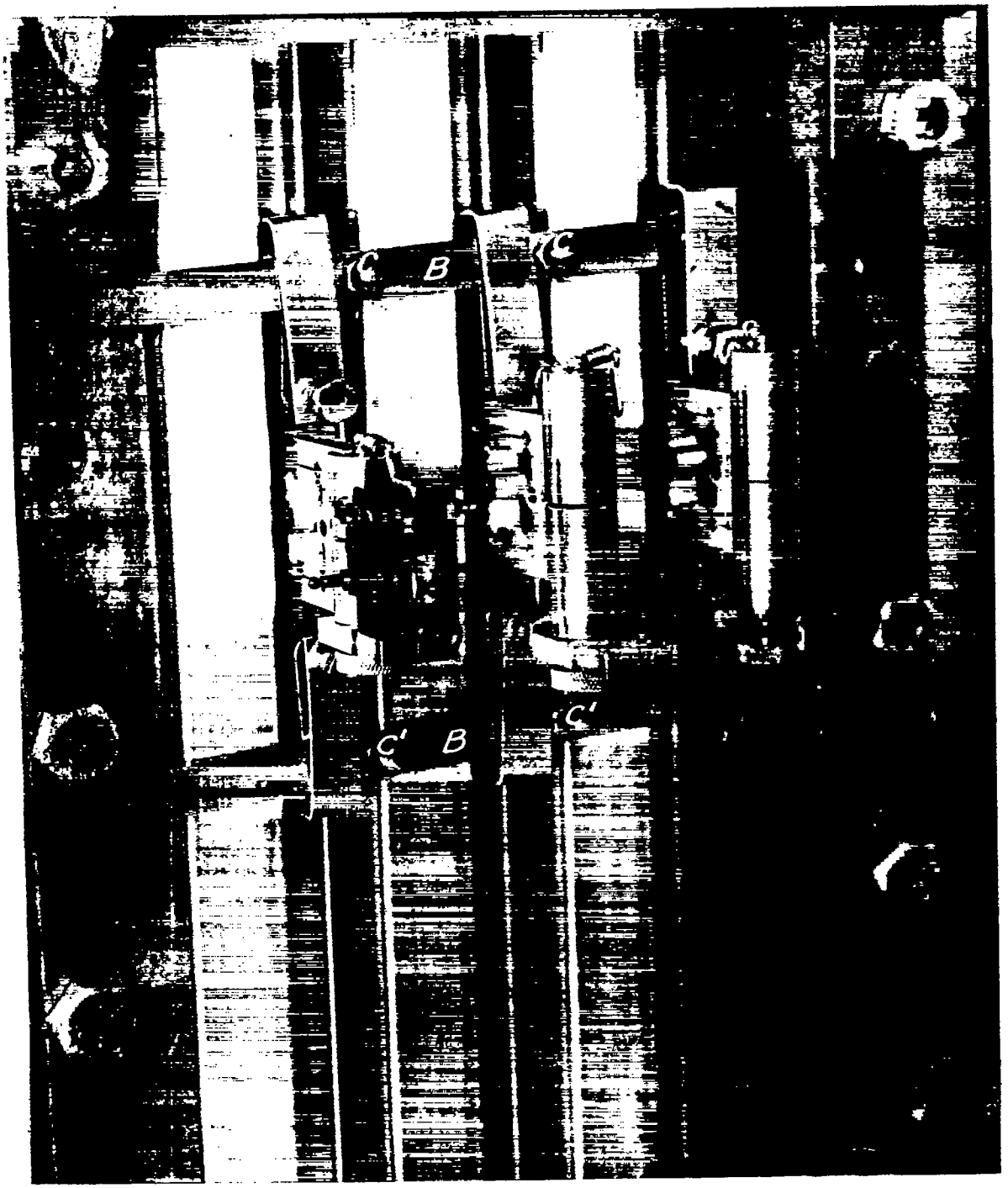

Figure 11. - Meisse transfers mounted on stringers, panel 3.

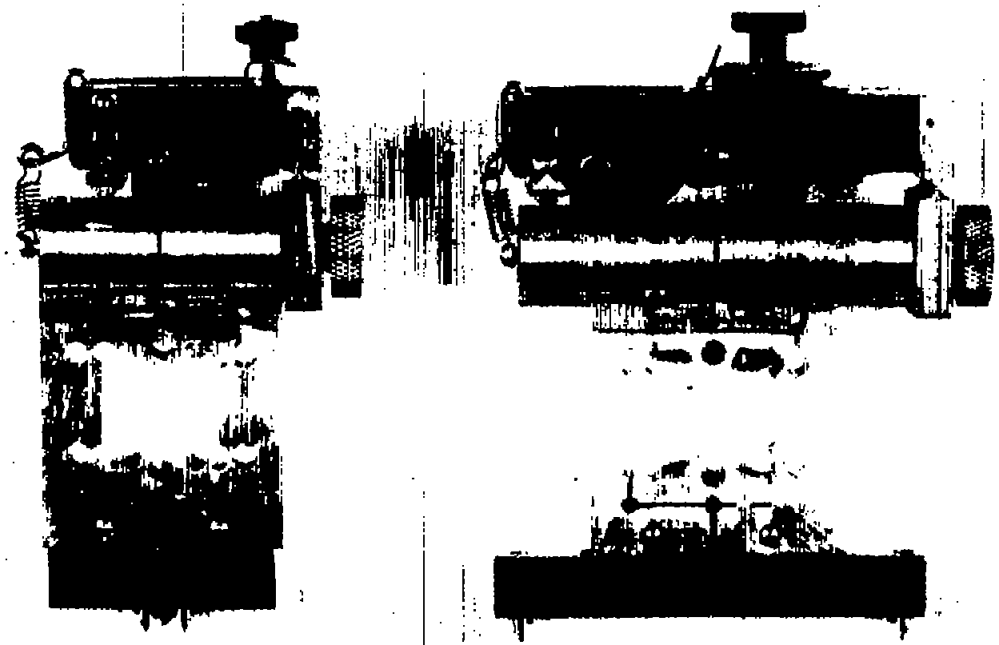

Figure 12. - Meisse transfer and Tuckerman strain gage for 0.2 - and 2-inch gage lengths.

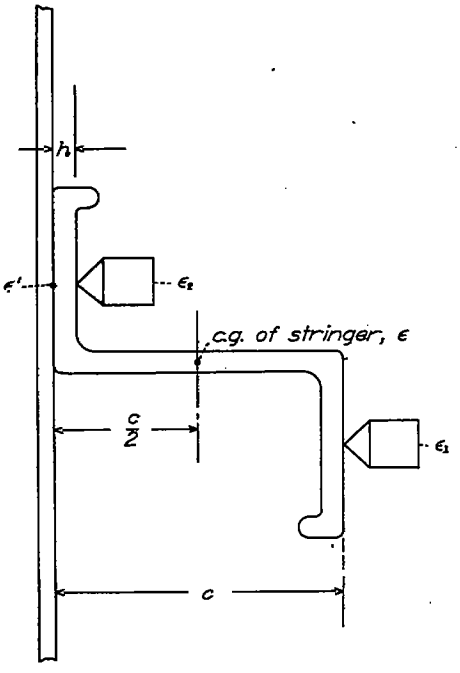

Figure 13.- Strain Measurements on stringers.

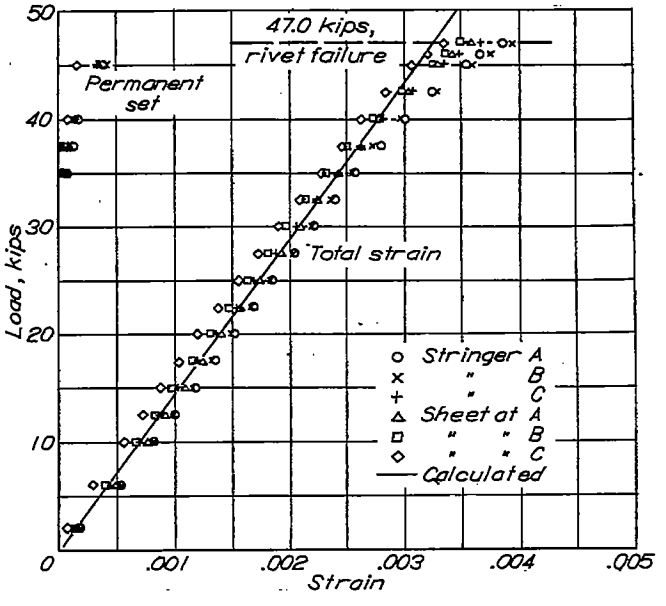

Figure 16.- Test of panel 1; b/t = 20.0, L/t = 20.0.

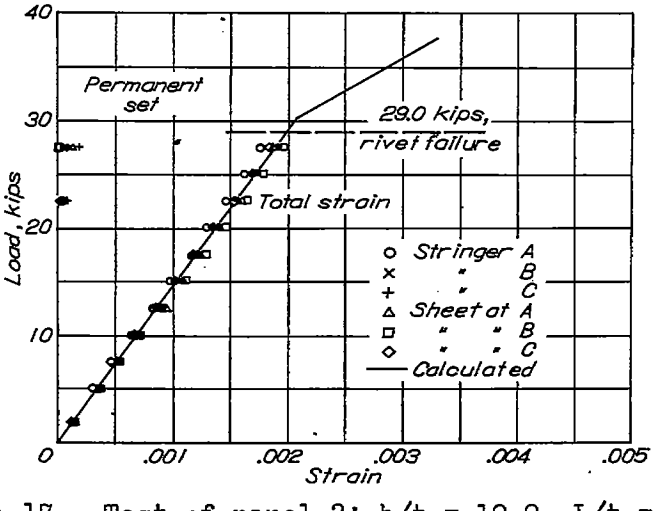

Figure 17.- Test of panel 2; b/t = 19.9, L/t = 39.7.

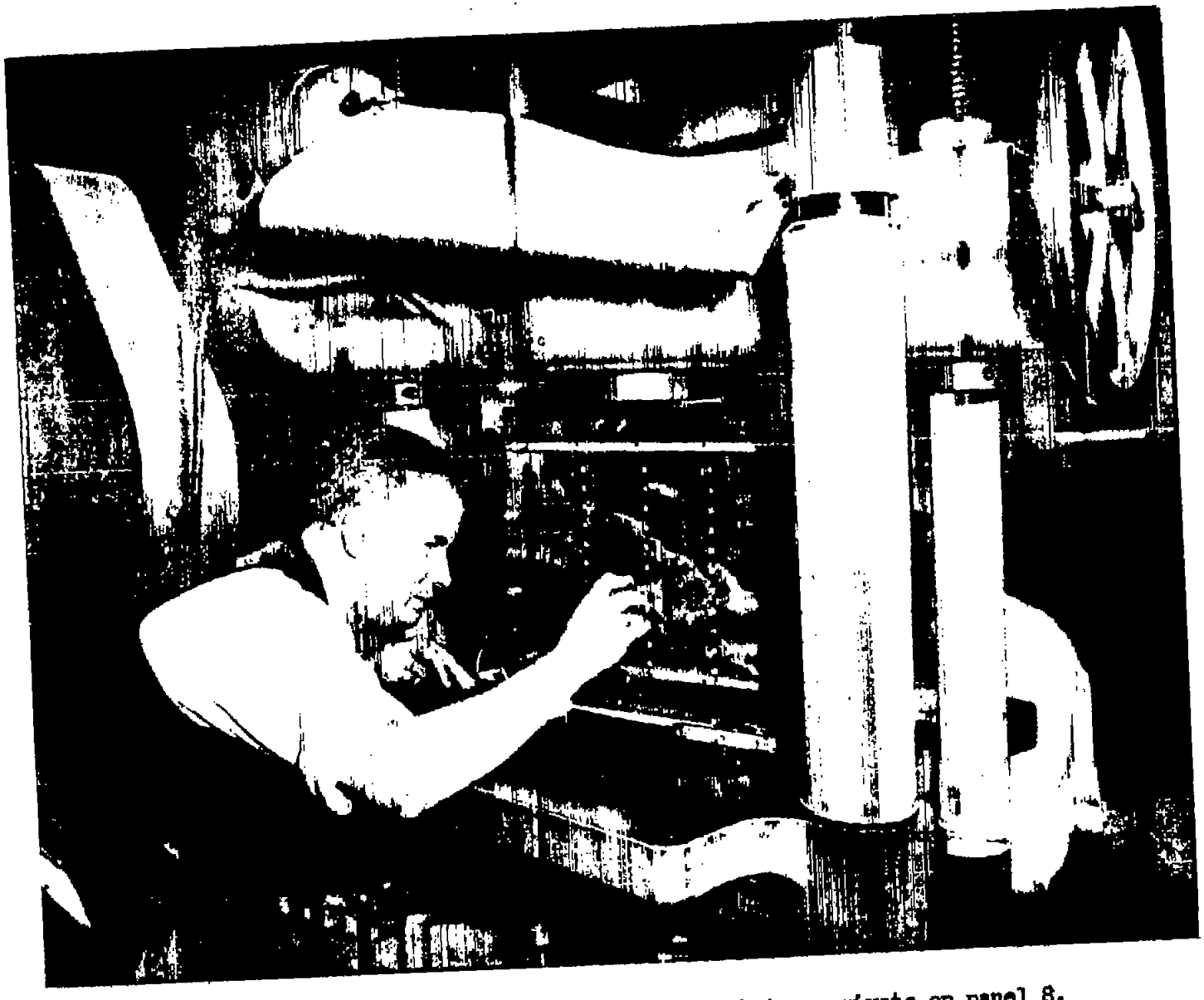

Figure 14. - Measurement of sheet deflection between rivets on panel 8.

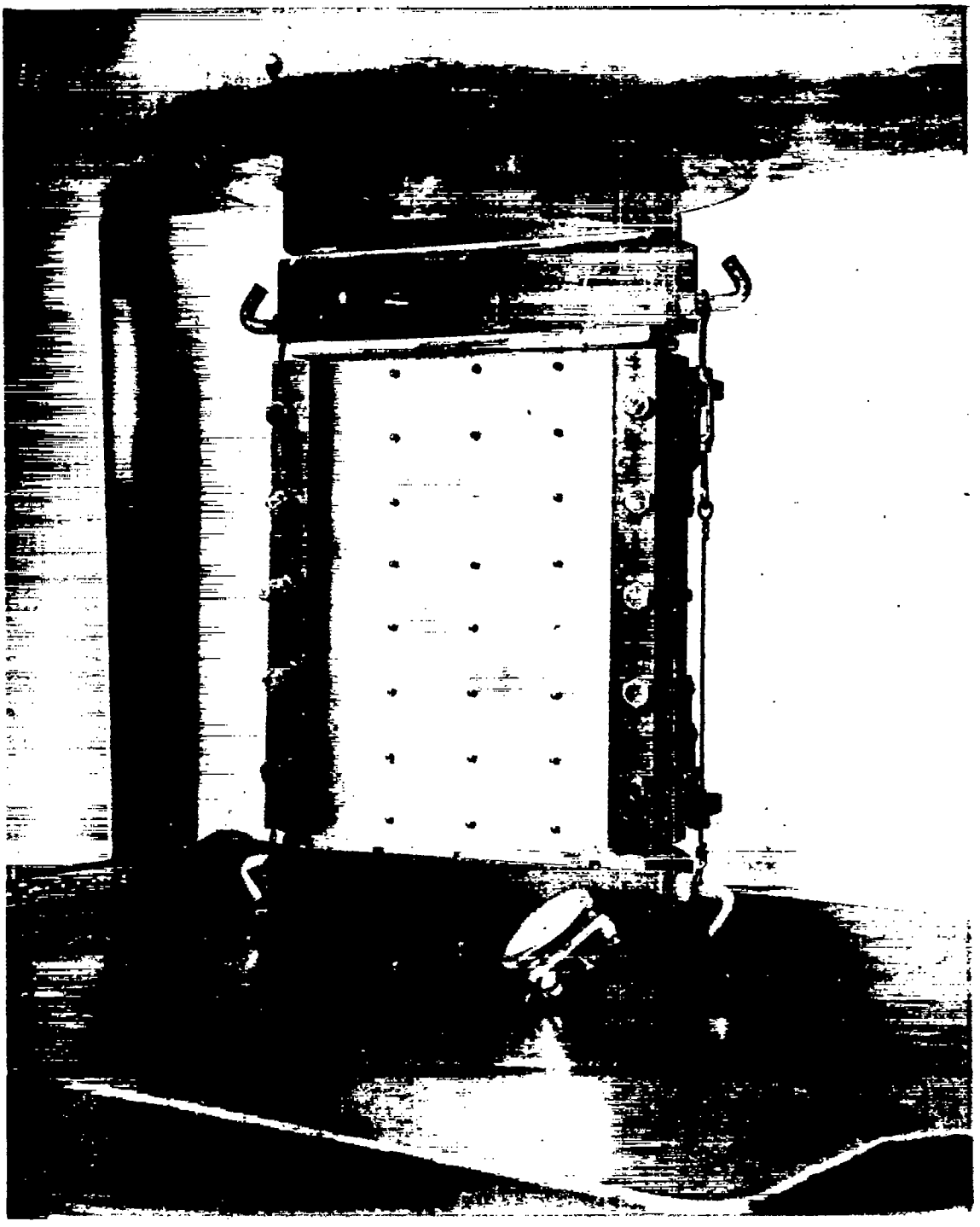

Figure 15. - Panel 15 after test.

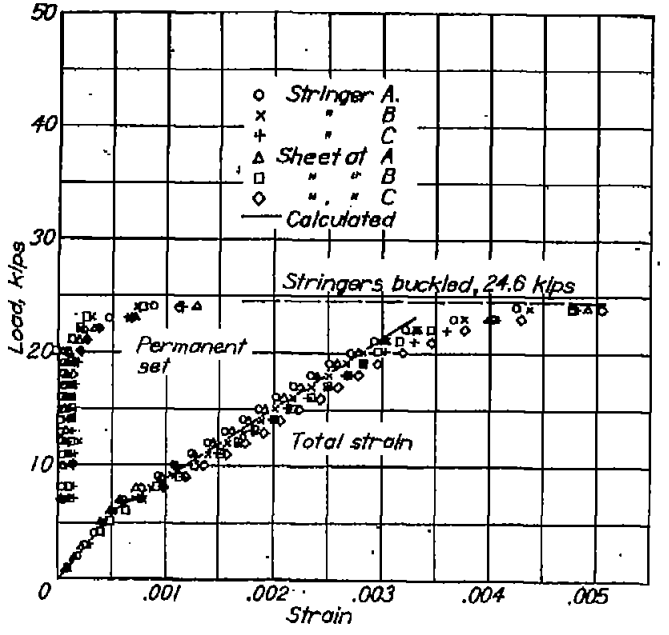

Figure 18.- Test of panel 3; b/t = 19.0, L/t = 76.1.

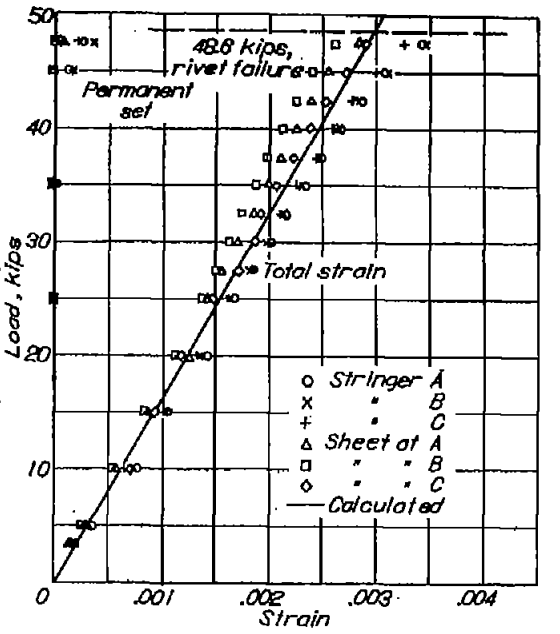

Figure 19.- Test of panel 4; b/t = 37.9, L/t = 19.0.

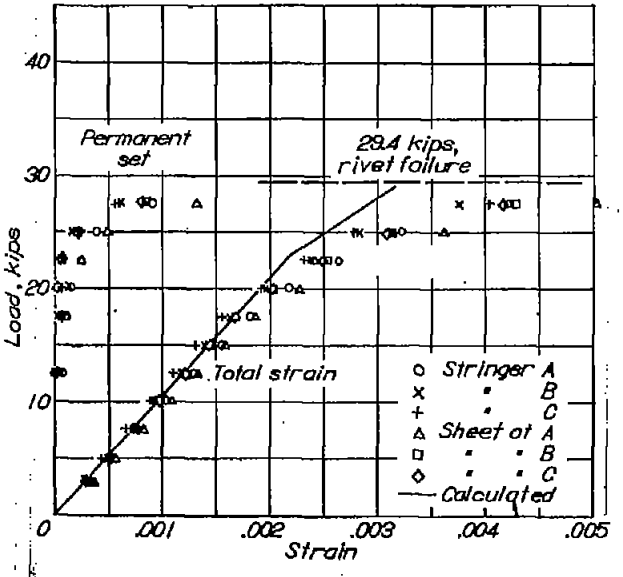

Figure 20.- Test of panel 5; b/t = 39.1, L/t = 39.1.

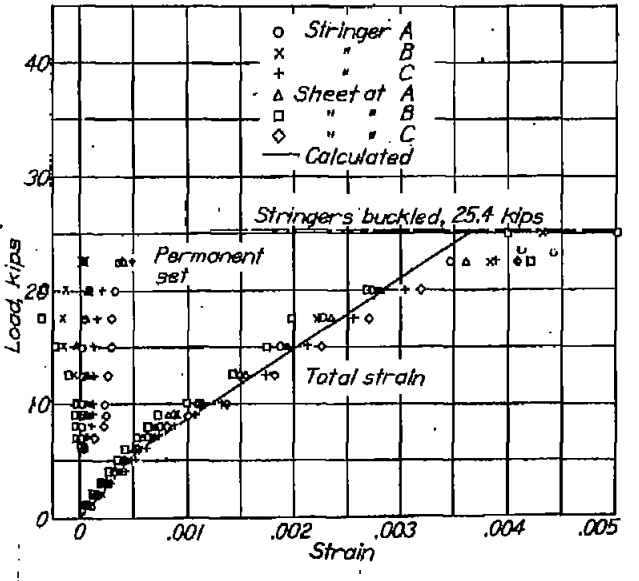

Figure 21.- Test of panel 6; b/t = 38.6, L/t = 77.3.

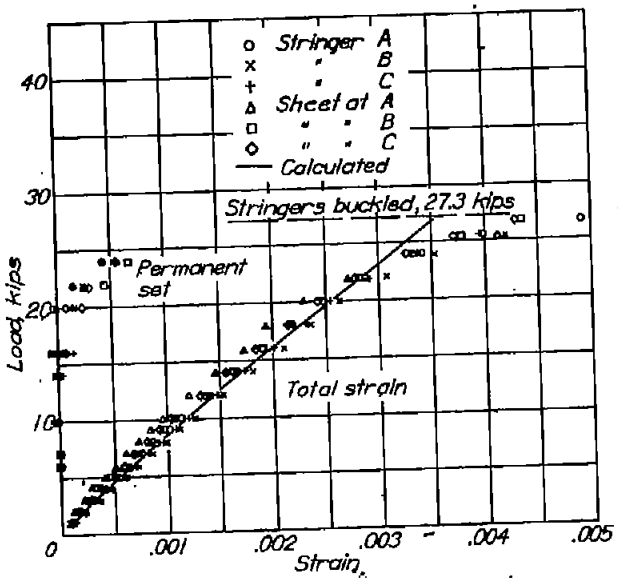

Figure 22.- Test of panel 7; b/t = 161, L/t = 20.1.

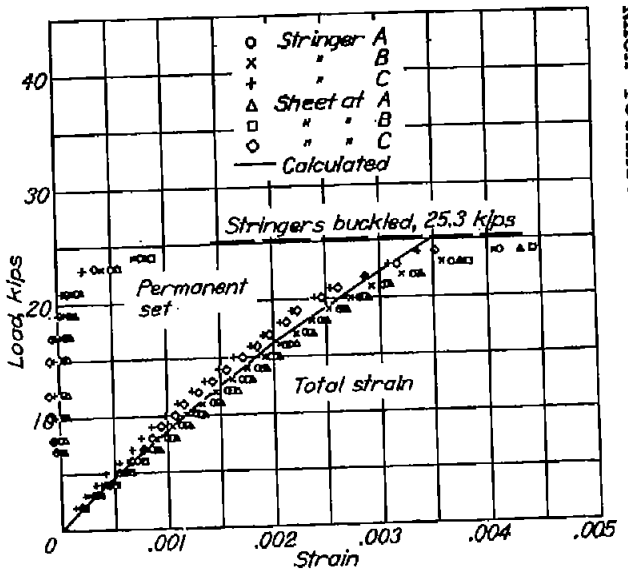

Figure 23.- Test of panel 8; b/t = 161, L/t = 40.2.

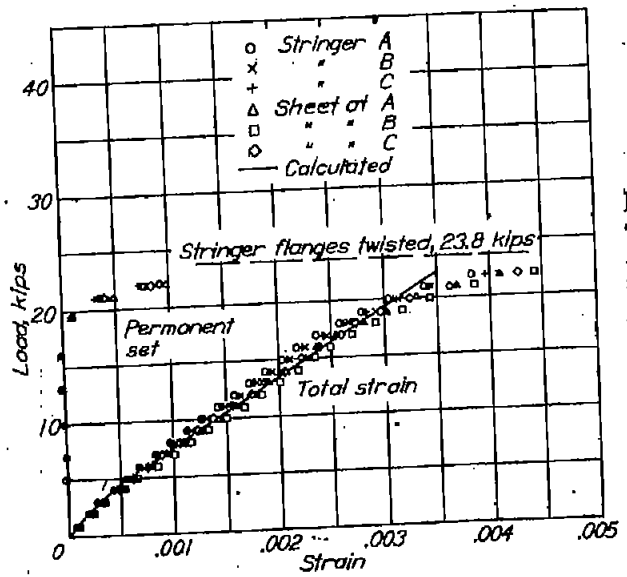

Figure 24.- Test of panel 9; b/t = 162, L/t = 80.9.

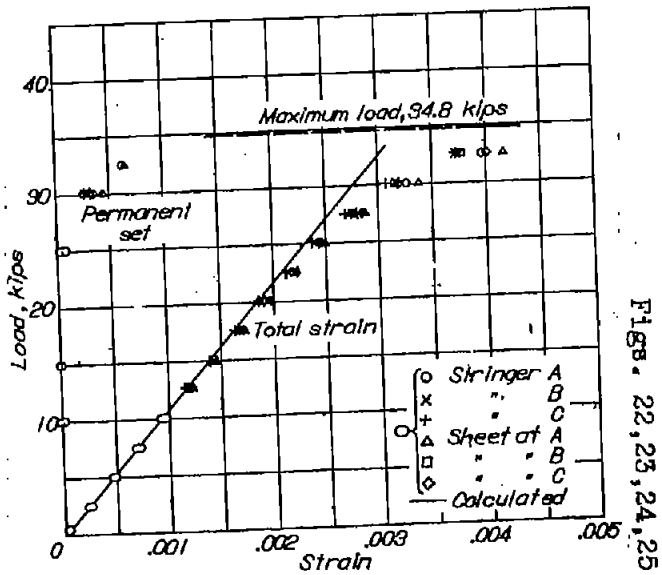

Figure 25.- Test of panel 13; b/t = 39.4, L/t = 9.86.

Figs. 22, 23, 24, 25

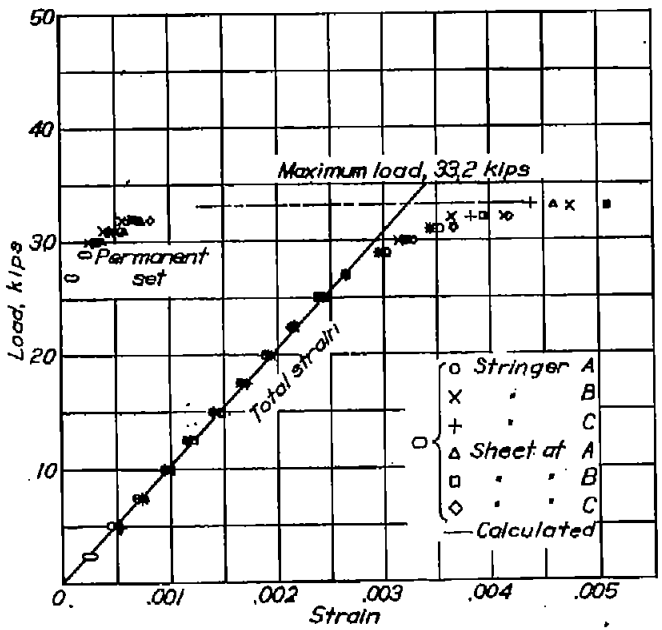

Figure 26.- Test of panel 14; b/t = 39.8, L/t = 19.9.

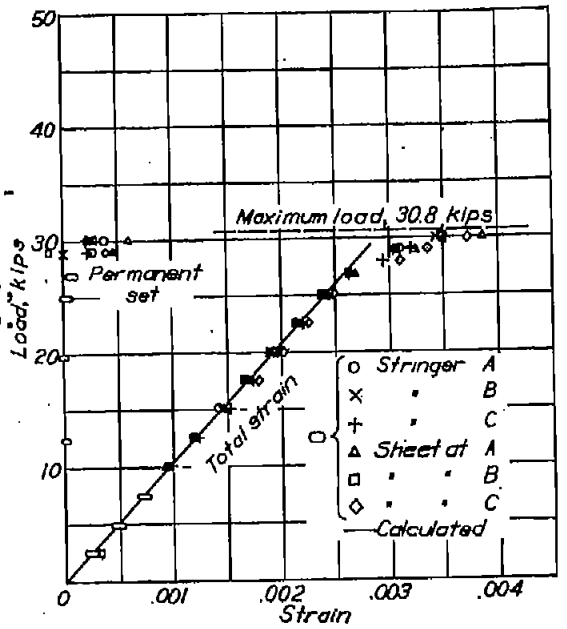

Figure 27.- Test of panel 15; b/t = 39.0, L/t = 29.3.

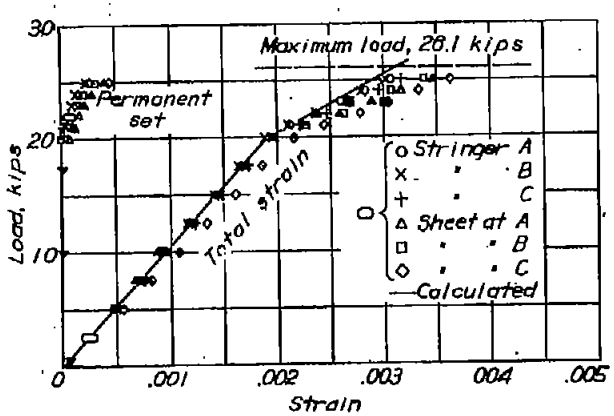

Figure 28.- Test of panel 16; b/t = 39.8, L/t = 39.8.

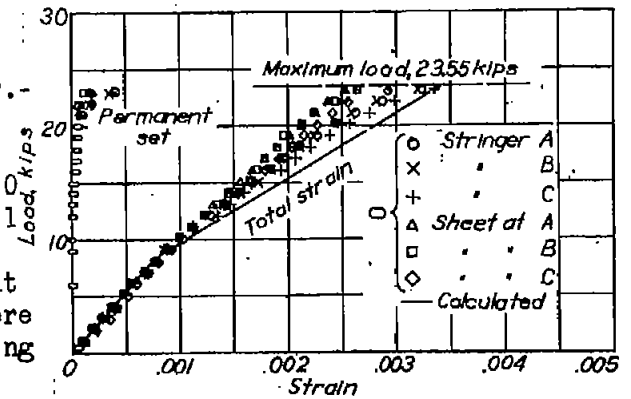

Figure 29.- Test of panel 17; b/t = 40.0, L/t = 60.1. Gages located at point where no buckling occurred.

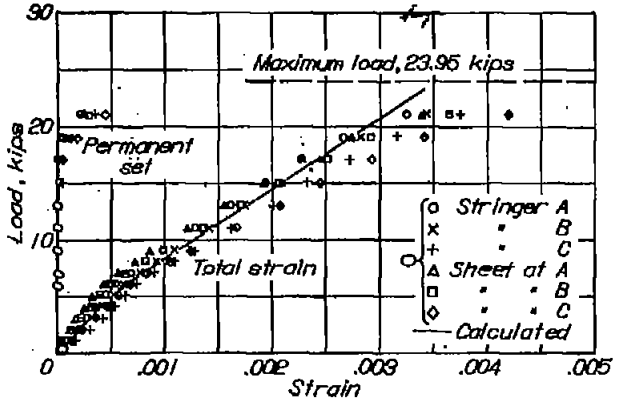

Figure 30.- Test of panel 18; b/t = 40.1, L/t = 80.0.

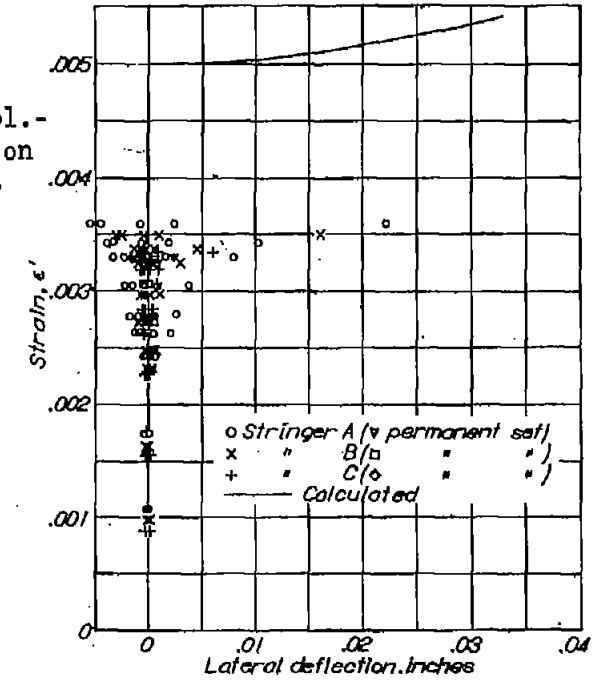

Figure 31.- Deflection of sheet between rivets, panel 1.

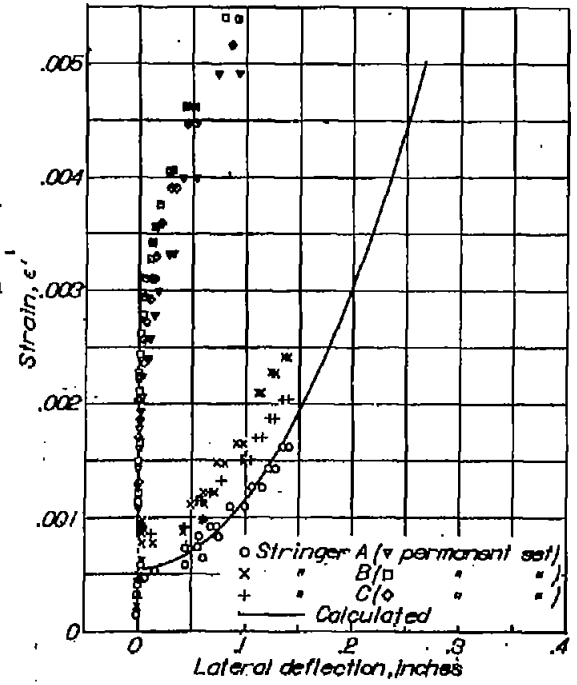

Figure 33.- Deflection of sheet between rivets, panel 3.

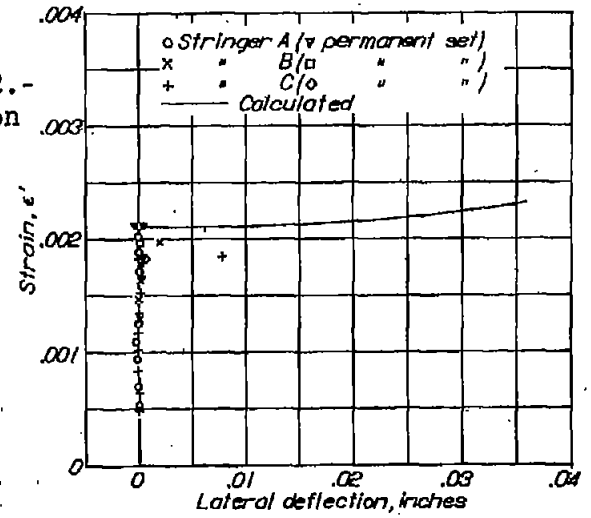

Figure 32.- Deflection of sheet between rivets, panel 2.

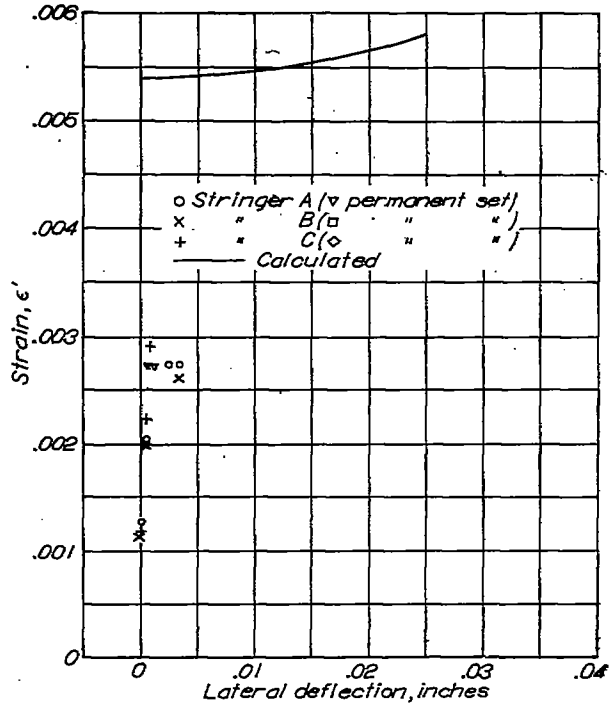

Figure 34.- Deflection of sheet between rivets, panel 4.

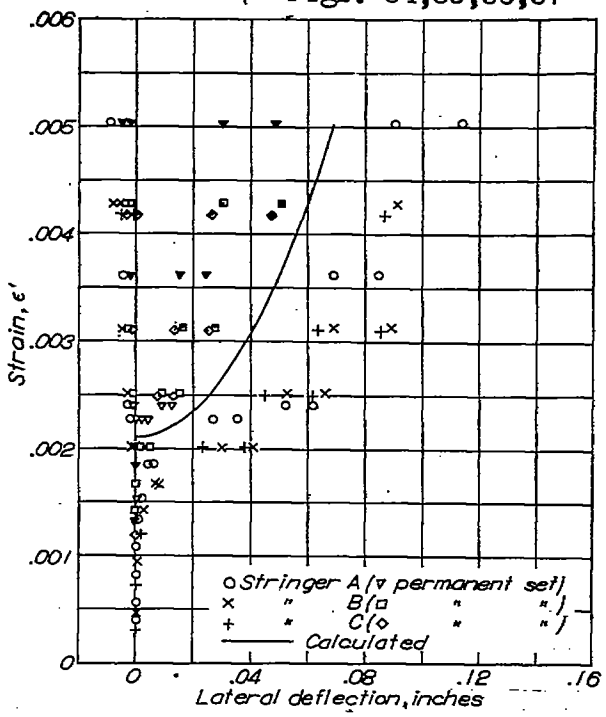

Figure 35.- Deflection of sheet between rivets, panel 5.

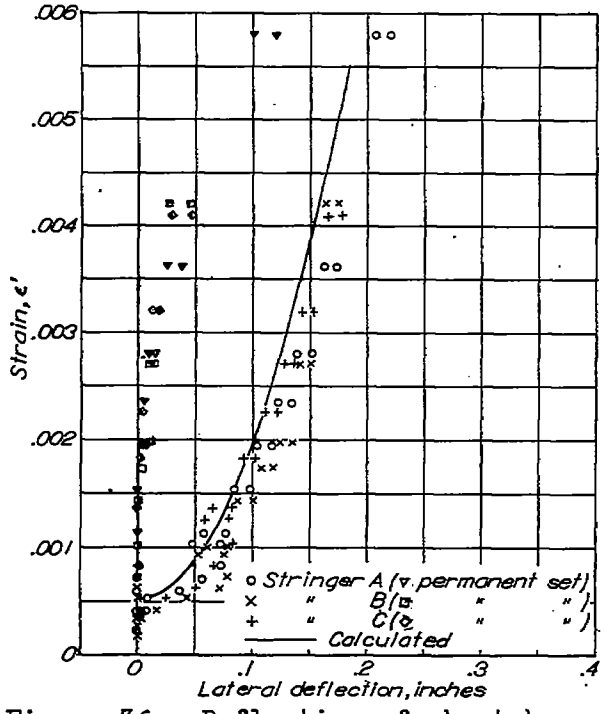

Figure 36.- Deflection of sheet between rivets, panel 6.

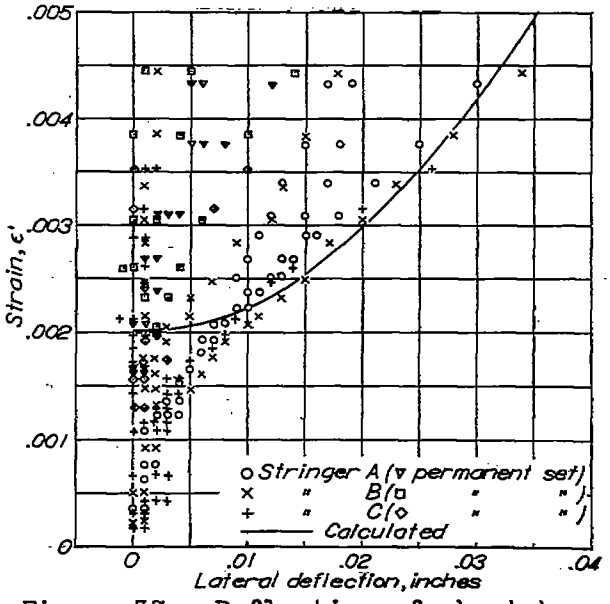

Figure 37.- Deflection of sheet between rivets, panel 8.

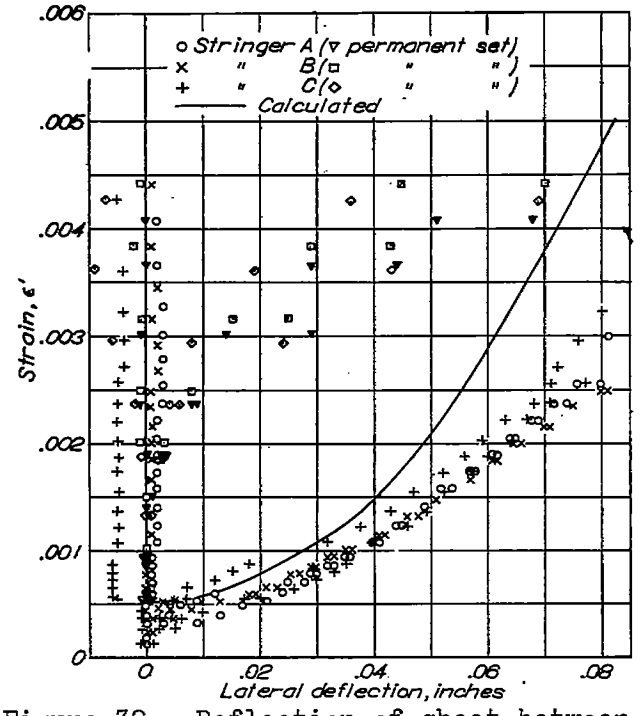

Figure 38.- Deflection of sheet between rivets, panel 9.

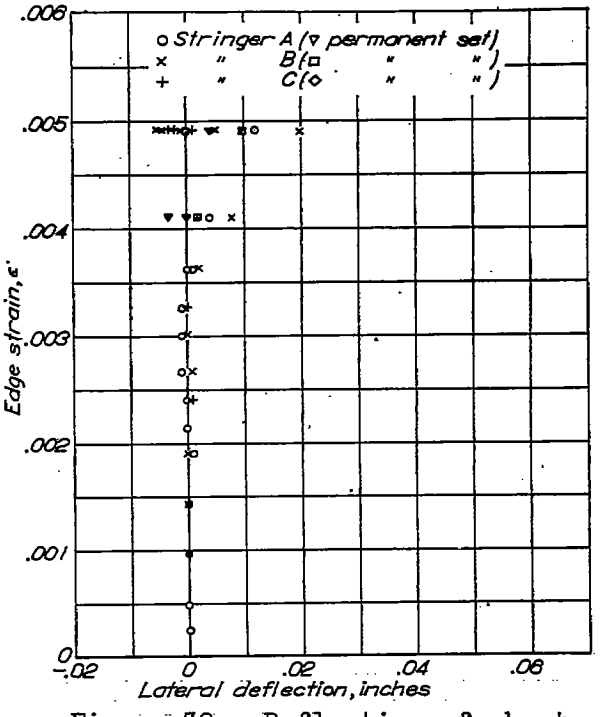

Figure 39.- Deflection of sheet between spot-welds, panel 14.

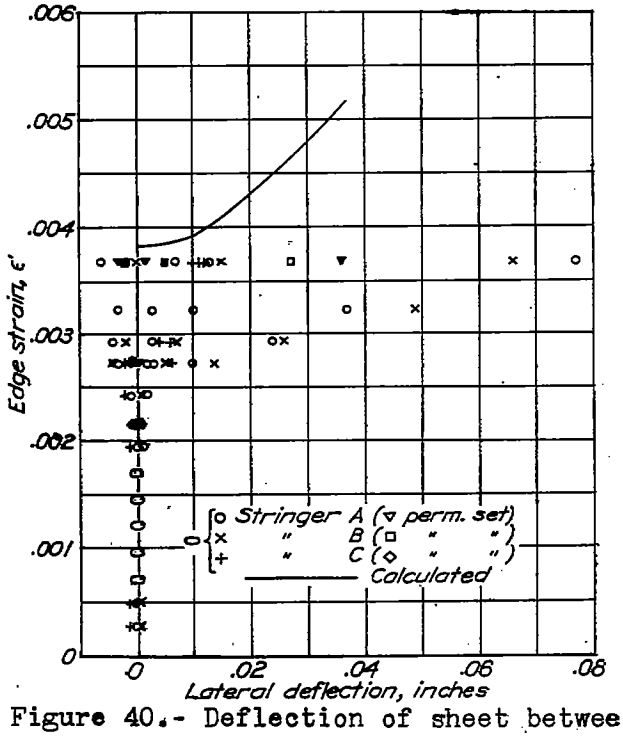

Figure 40.- Deflection of sheet between spot-welds, panel 15.

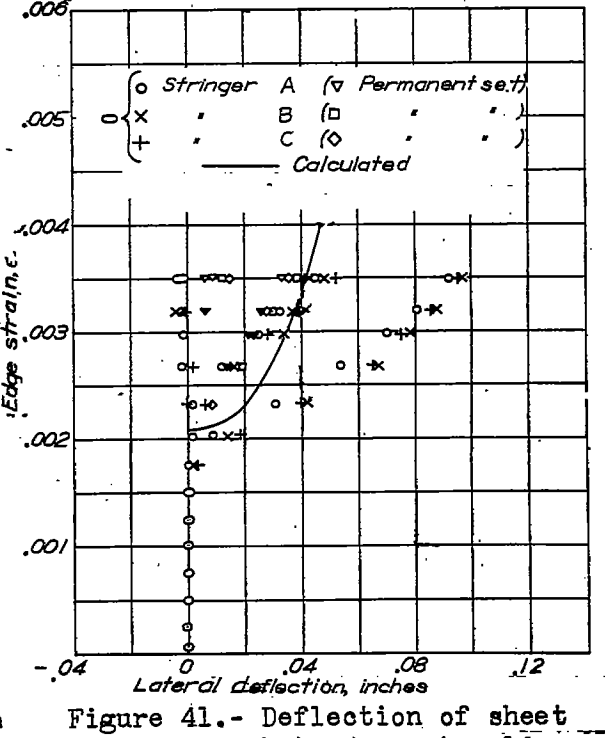

Figure 41.- Deflection of sheet between spot-welds, panel 16.

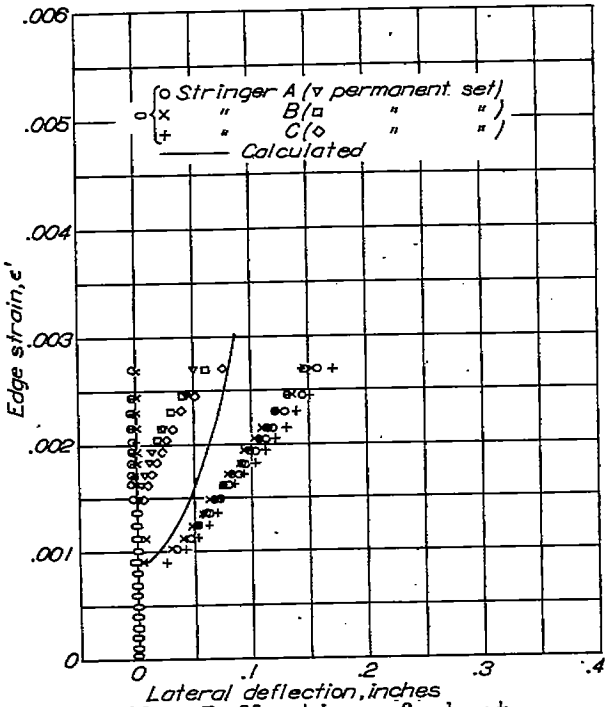

Figure 42.- Deflection of sheet between spot-welds, panel 17.

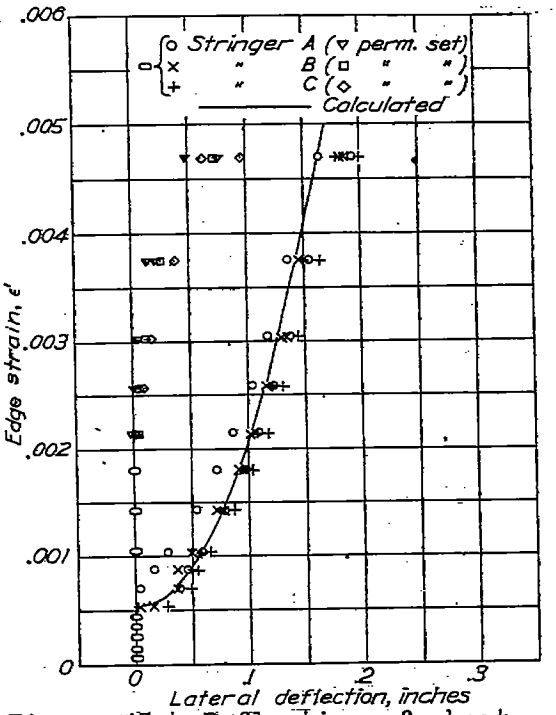

Figure 43.- Deflection of sheet between spot-welds, panel 18.

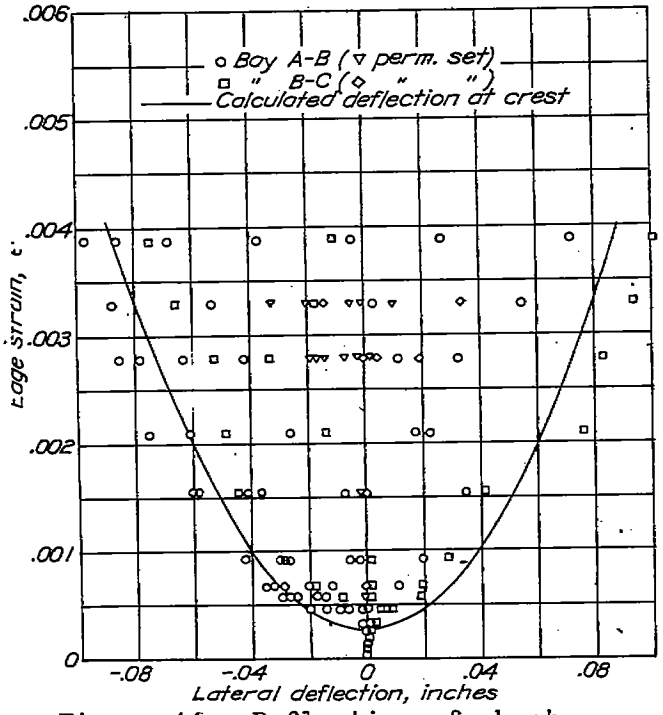

Figure 44.- Deflection of sheet between stringers, panel 7.

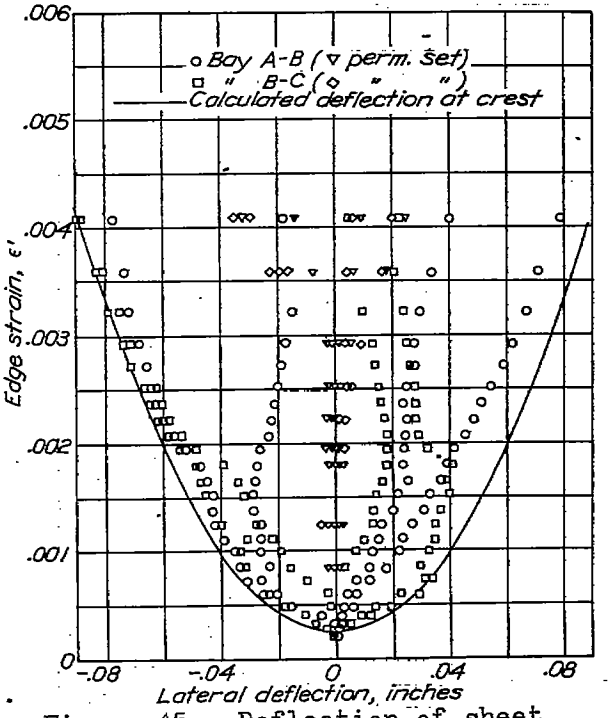

Figure 45.- Deflection of sheet between stringers, panel 8.

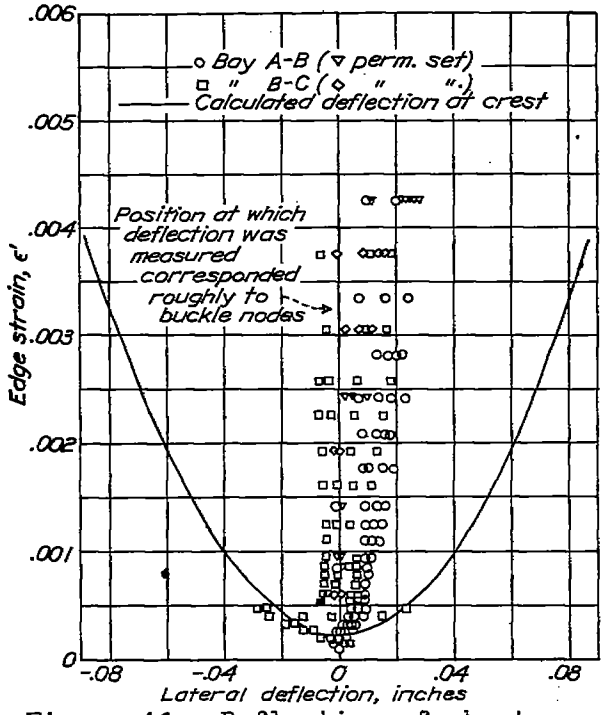

Figure 46.- Deflection of sheet between stringers, panel 9.

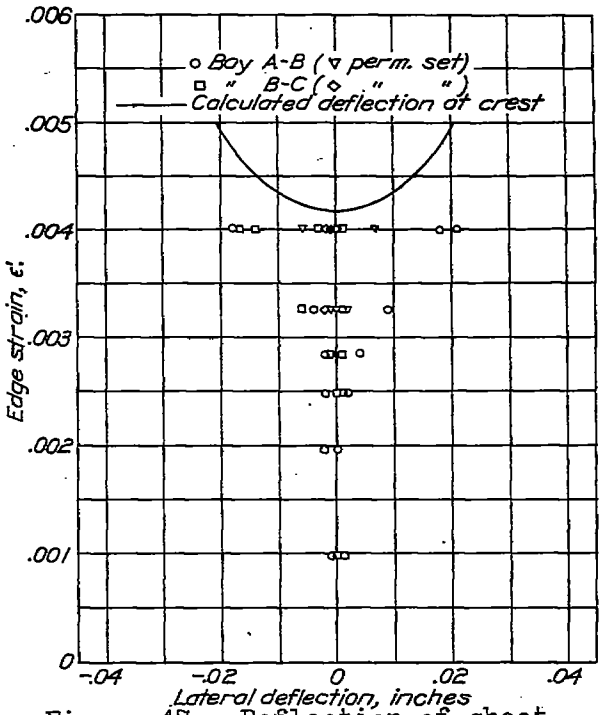

Figure 47.- Deflection of sheet between stringers, panel 13.

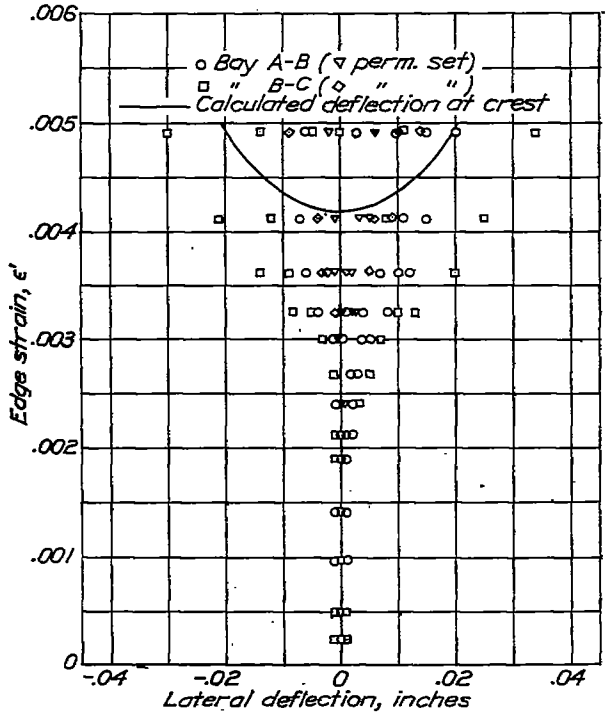

Figure 48.- Deflection of sheet between stringers, panel 14.

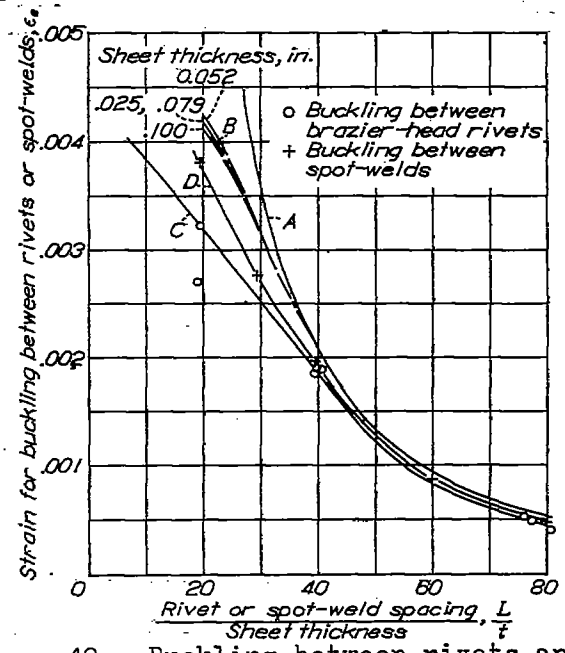

Figure 49.- Buckling between rivets and spot-welds: curve A, elastic buckling strain (eq. 3); curve B, buckling strain above proportional limit; curve C, experimentally obtained with brazier-head rivets; and curve D, experimentally obtained with spot-welds.

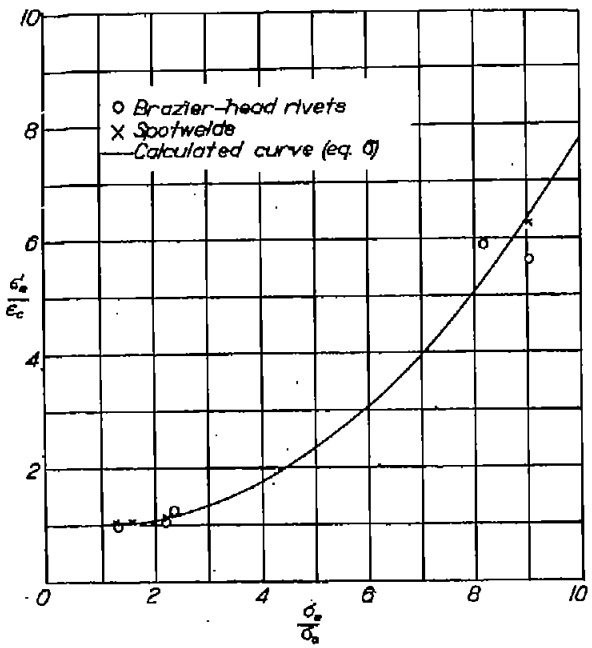

Figure 50.- Strain for permanent set in buckles between rivets or spot-welds. ϵ_c = buckling strain; ϵ'_s = strain at sheet side of stringer for permanent set in buckle; σ_c = buckling stress corresponding to ϵ_c (see fig. 2); and σ_s = compressive yield strength (0.002 offset) of sheet (table 2).

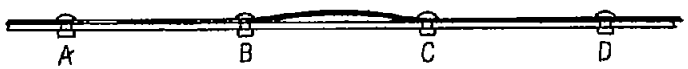

Buckling between rivets in panel 5 near failure (.5 actual size)

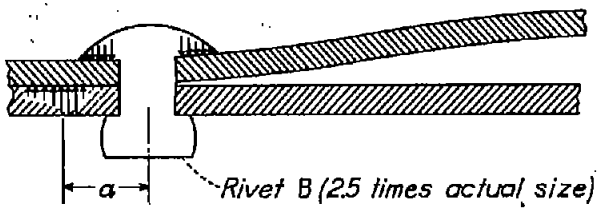

Figure 53.- Buckling between rivets in panel 5.

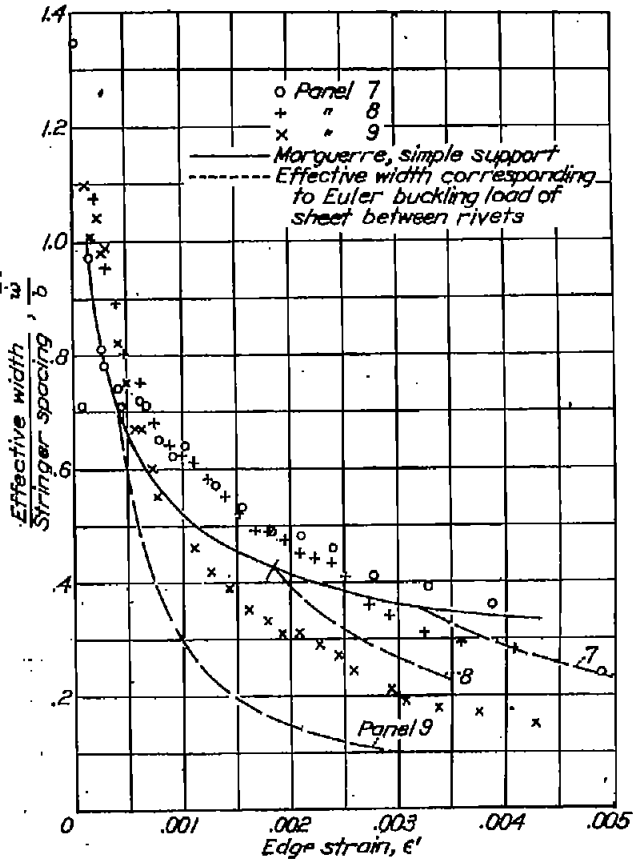

Figure 54.- Comparison of effective width of panels 7,8, and 9 with theoretical values.

Figs. 50, 53, 54

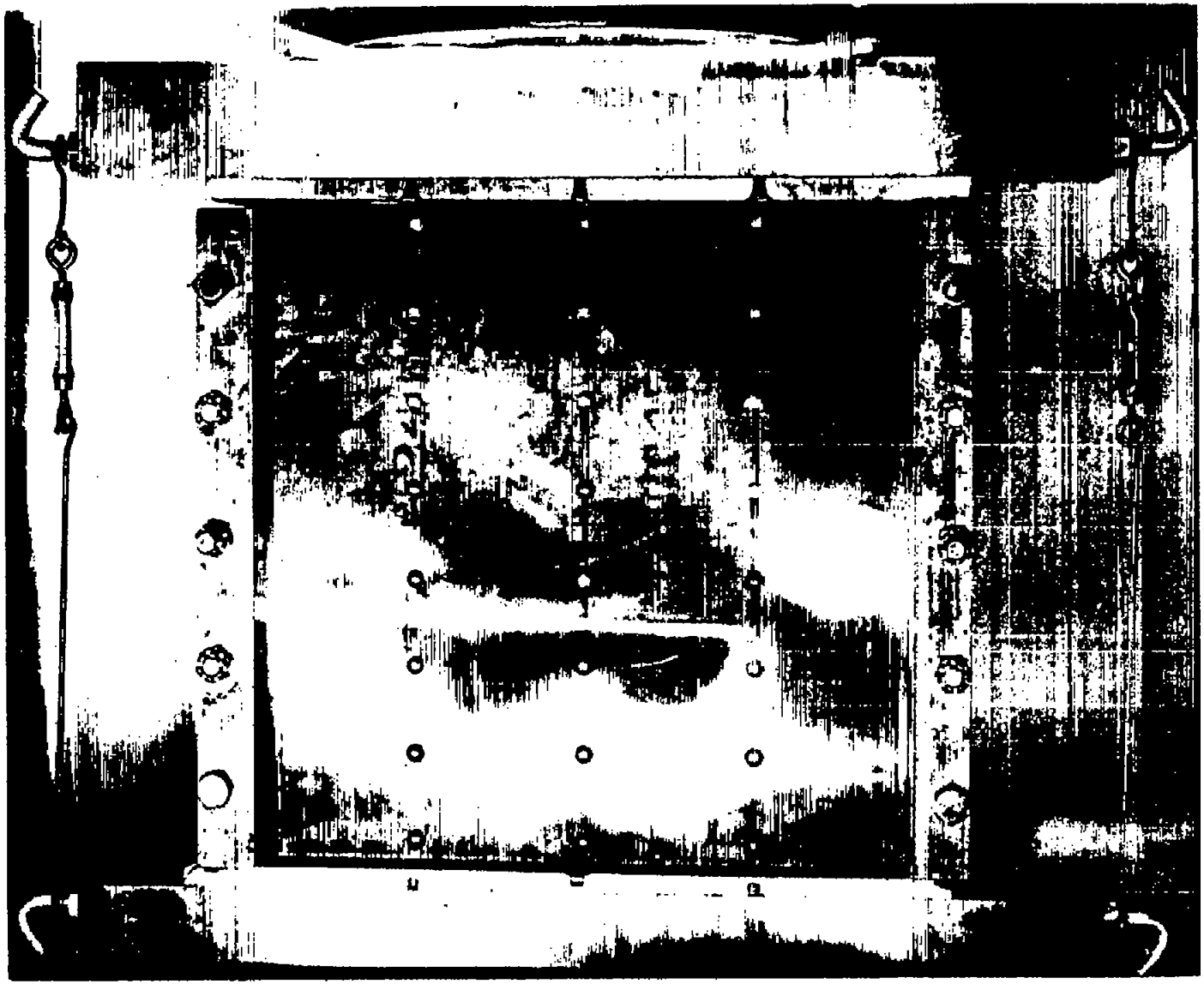

Figure 51. - Panel 4 under a load of 48 kips.

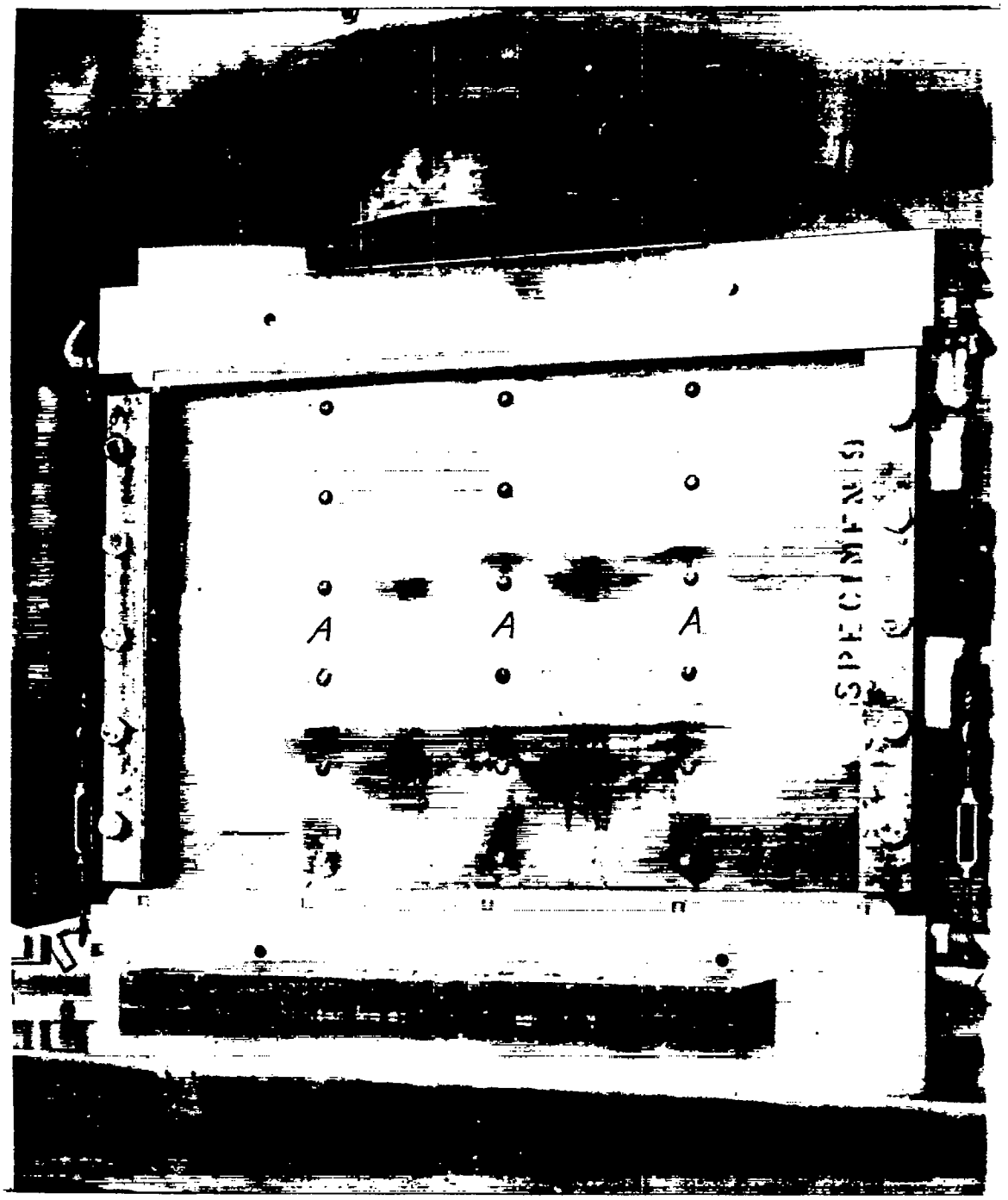

Figure 52. - Panel 9 after test.

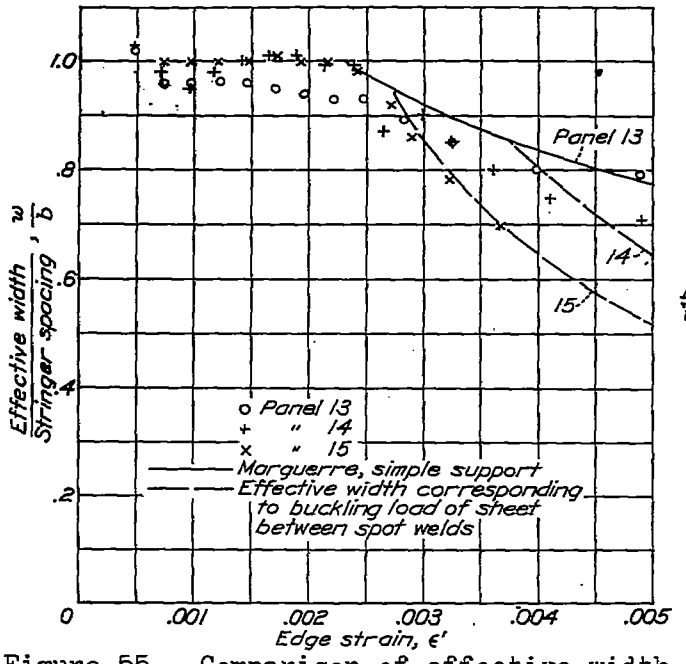

Figure 55.- Comparison of effective width of panels 13,14, and 15 with theoretical values.

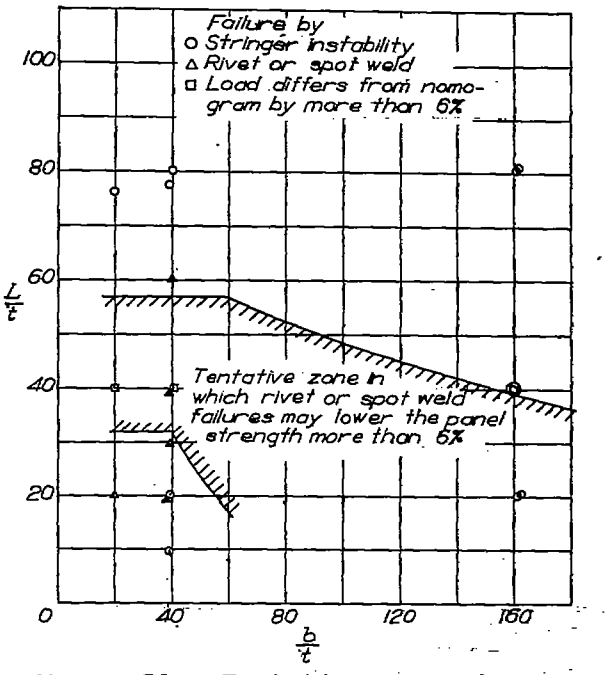

Figure 59.- Tentative zone where the strength of panels of the type tested may be lowered more than 6 percent by rivet or spot-weld failure.

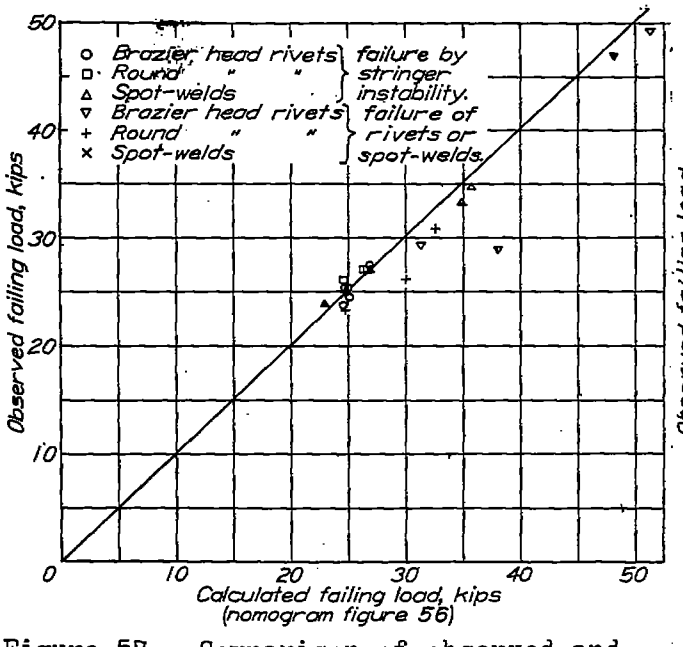

Figure 57.- Comparison of observed and calculated failing load for 18 panels tested.

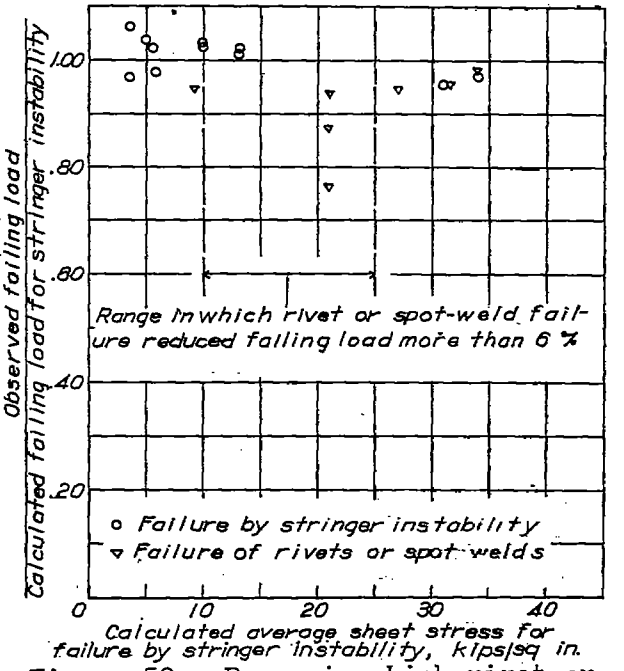

Figure 58.- Range in which rivet or spot-weld failure is likely to occur.

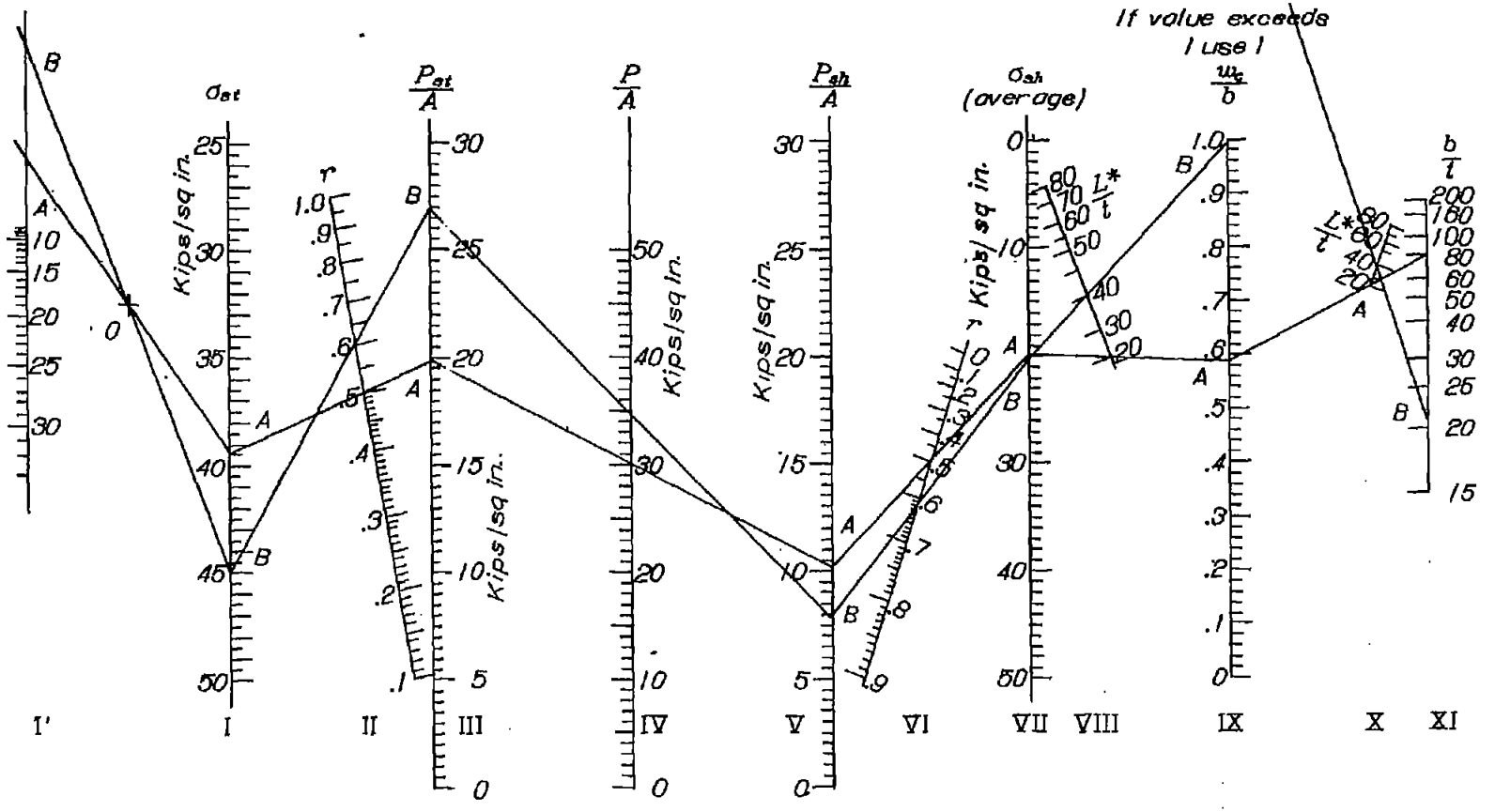

Figure 56.- Nomogram for 24S-T aluminum-alloy panels of design given in figure 1 which fail by stringer instability.

σ_{st}	Stress in stringer at failure	P/A	Average stress in panel
r	Reinforcement ratio	σ_{sh}	Average sheet stress at failure
L/t	Rivet spacing over sheet thickness	*	Intercept on scale I' used here if greater than L/t
b/t	Stringer spacing over sheet thickness		

w_c/b = ratio of effective width to stringer spacing

Fig. 56